

Accounts**Design, Synthesis, Structure, and Spectroscopic and Electrochemical Properties of Phthalocyanines****Nagao Kobayashi**

Department of Chemistry, Graduate School of Science, Tohoku University, Sendai 980-8578

(Received July 31, 2001)

The synthesis and spectroscopic and electrochemical properties of crown-ether substituted metallophthalocyanines (MCRPcs), optically active phthalocyanines (Pcs), subphthalocyanines (SubPcs), low symmetrical Pcs, ring-expanded Pcs, and novel oligomers of Pcs studied mainly by the author over the last 20 years have been reviewed, together with the electrocatalytic reduction of dioxygen using water soluble Pcs. MCRPcs form, on addition of certain kinds of cation, co-facial dimers through a two-step three-stage process. SubPcs react with isoindolediimines to produce mono-substituted Pc and Pc analogues. Optically active Pcs have been prepared to show the beauty and usefulness of circular dichroism spectroscopy. Ring-expanded or -shrunk and low symmetrical Pc analogues have helped in exploiting the relationship between size, symmetry, and spectroscopic and electrochemical properties of large aromatic molecules. Molecular orbital calculations on these compounds have succeeded in reproducing many of the experimental properties. New types of cofacial and planar dimers have been prepared, occasionally with a new concept. Water-soluble iron and cobalt Pcs electrocatalyze the reduction of dioxygen. When a four-electron reduction was attained, the reduction proceeded via hydrogen peroxide, and could be explained by a mechanism of electrochemical catalyst regeneration. The results for these compounds are occasionally compared with those of porphyrin systems.

Phthalocyanines (Pcs) are a robust and versatile class of compounds. The first accidental synthesis was reported in 1907,¹ and one of its structures was confirmed by X-ray crystallography in 1936.² Although they are relatives of porphyrins, **1** (Fig. 1), Pcs and particularly metalloPcs (MPcs), **2**, are much more planar than metalloporphyrins. They have been firmly established as blue and green dyestuffs and pigments, catalysts for sulfur-removing processes in the oil industry, deodorants, and germicides, while their recent use as photoconducting agents in photocopying machines has provoked research in various fields, including chemical sensors, electrochromism, photodynamic reagents for cancer therapy and other medical applications, photovoltaic cell elements for electricity generation, electrophotography, optical computer read/write discs, low-dimensional metals, non-linear optics, electrocatalysis, liquid crystals, and Langmuir–Brodgett films.^{3,4} At present, more than 50000 tons of Pcs are produced per year across the world. Most of these applications are concerned with the large, flat π -conjugation system of Pcs, as well as with the type of central metal. However, the work on soluble Pcs was limited when I started research work on Pcs about 20 years ago, and most of the results had been published only as patents. Another hindrance to Pc research compared with porphyrin research was the fact that molecular design is more difficult, because stepwise synthesis is generally almost impossible (MPcs are generally obtained in one-step by a template reaction using

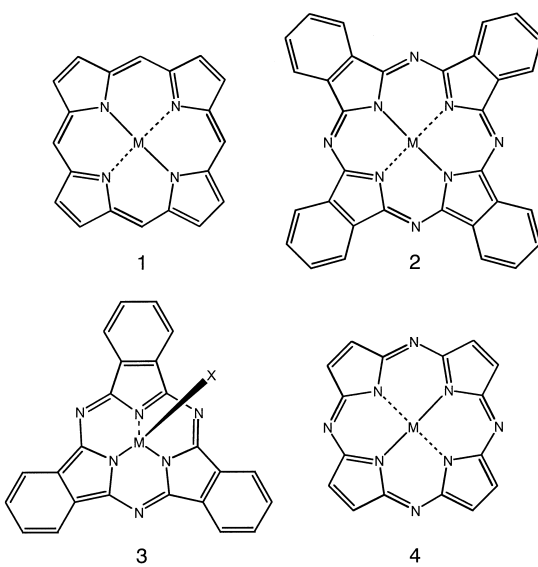


Fig. 1. Basic structures of general metalloporphyrin **1**, metallophthalocyanine **2**, subphthalocyanine **3**, and tetraaza-porphyrin **4**.

metal ions). My Pc research began with the preparation of solvent soluble Pcs.

1. Crown Ether-Substituted Phthalocyanines

The chemistry of crown-ether-substituted porphyrins was started for the first time by us in 1981.⁵ Since then, a large amount of data has been accumulated.⁶ On the other hand, the first report on crown-ether substituted Pcs appeared independently from three groups in 1986.⁷ Fortunately, the compound was the same, 15-crown-5-ed CuCRPc, and in addition, the journal was also the same. The most notable points about this type of compound were in the process of dimerization in the presence of cations, and the resultant cofacial eclipsed structure. Dimerization in the presence of K^+ was first pursued in detail using absorption spectroscopy (Fig. 2A).⁸ In the

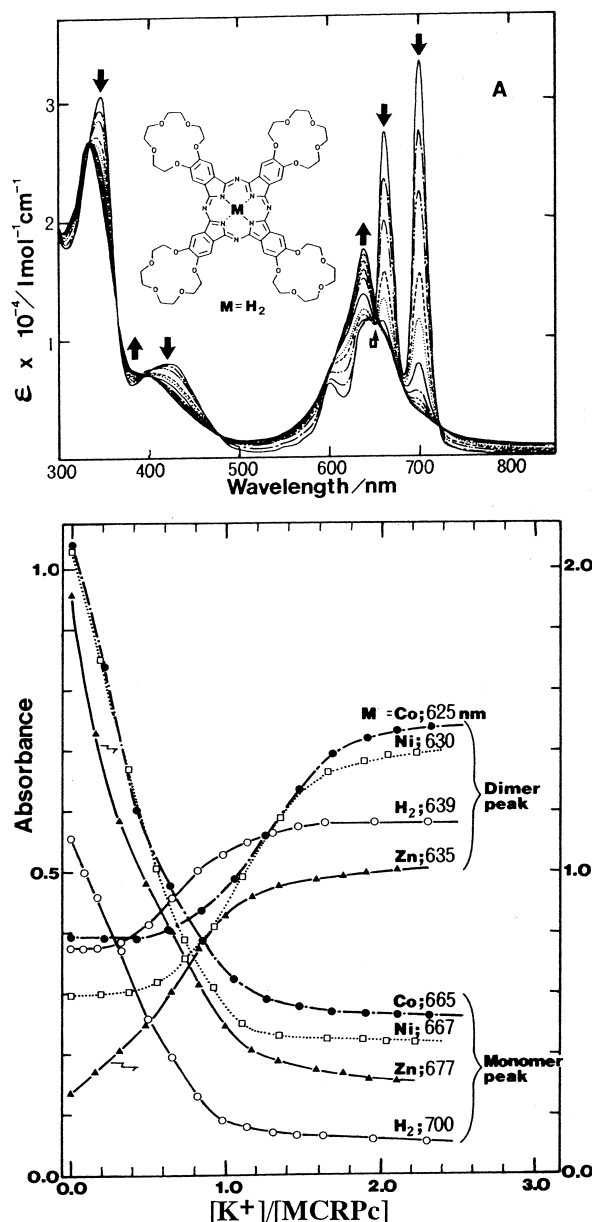


Fig. 2. (A) Change of absorption spectra of H_2 CRPc by the addition of CH_3COOK in $CHCl_3$. (B) The dependence of absorbance of several MCRPc's on $[K^+]/[MCRPc]$ at several wavelengths.

region where $0 < [K^+]/[MCRPc] < 0.5$, a set of isosbestic points was observed between the spectra of monomeric MCRPc in the absence and presence of cations. However, in the region ca. $0.5 < [K^+]/[MCRPc] < 1.5$ –2.0, another set of isosbestic points was detected with the spectrum at ca. $[K^+]/[MCRPc] = 0.5$. During this process (Fig. 2B), the Q band of monomeric MCRPc faded away and concomitantly a new Q peak developed at shorter wavelengths (Fig. 2A). Since this type of spectrum is expected upon cofacial stacking of chromophores,⁹ the EPR spectrum of CuCRPc at ca. $[K^+]/[CuCRPc] = 2$ –3 was recorded. From the characteristic spectrum for triplet species (Fig. 3), the Cu–Cu distance was estimated to be ca. 4.1–4.2 Å. In addition, 1H NMR spectra of Zn- and H_2 CRPc were compared in the absence and presence of K^+ . Compared with the spectrum in the absence of cations, proton signals in the crown ether unit shifted downfield to varying extents, while the pyrrole proton signal shifted inversely to higher field from -3.41 to -8.09 ppm at $[K^+]/[MCRPc] = 2$ –3. Monomeric H_2 - and ZnCRPc showed fluorescent emission from the lowest π – π^* (Q band) state, at around 700 nm. Similarly to the absorption spectra, the fluorescence was little changed in the range $0 < [K^+]/[H_2$ - or ZnCRPc] < 0.5. However, in $0.5 < [K^+]/[MCRPc] < 1.5$, it was quenched significantly, and at ca. $[K^+]/[MCRPc] > 1.5$, its intensity was weakest. Interestingly, inflection points were detected clearly at ca. $[A^+]/[MCRPc] = 0.5, 1.0$, and 1.5 ($A^+ = K^+, Cs^+$), consistent with a stepwise capture of cations such as K^+ or Cs^+ . Thus, the above absorption, fluorescence emission, NMR, and EPR spectroscopies clearly showed a two-step three-stage dimerization. In the first step, two MCRPc capture one cation, such as K^+ or Cs^+ , at $0 < [K^+]/[MCRPc] < ca. 0.5$ to form a linear dimer, **5** (Fig. 4) which transforms to a cofacial dimer, **6**, by trapping the 2nd and 3rd cations at $0.5 < [K^+]/[MCRPc] < 1.5$, and at $ca. [K^+]/[MCRPc] > 1.5$ a cofacial dimer whose interplanar distance is ca. 4.1–4.2 Å is formed. Although not yet proven by X-ray crystallography, this cofacial dimer, **6** (Fig. 4), was considered to have a completely cofacial eclipsed

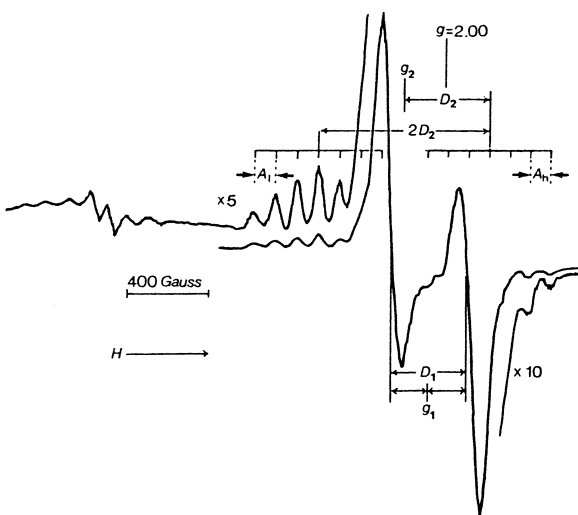


Fig. 3. EPR spectrum of CuCRPc in $CHCl_3$ – $MeOH$ (ca. 4:1 v/v) at 77 K in the presence of CH_3COOK ($[K^+]/[MCRPc] = 4$).

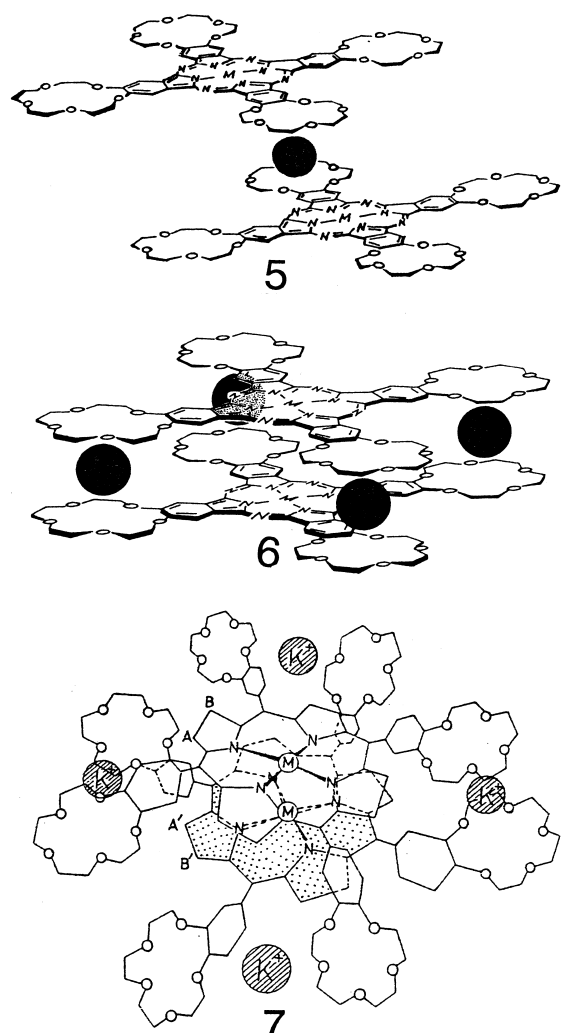


Fig. 4. Proposed structures for the cation-induced linear **5** and cofacial **6** dimer of MCRPc and a cofacial dimer of tetra-crowned metalloporphyrin **7**. Solid circles indicate cations such as K^+ and Ca^{2+} .

structure. Accordingly, the dimers were examined by various spectroscopic methods. Thus, both the electronic absorption and magnetic circular dichroism (MCD) spectra of cofacial dimeric H_2CRPc and NiCRPc have been analysed using a band deconvolution technique (Fig. 5, A–C).¹⁰ In this case, the spectral envelopes obtained from the same solution were fitted with the same number of bands and similar band centers and bandwidths, so that the ambiguity inherent in this type of analysis was reduced. For example, in the spectra of NiCRPc monomer, these bands were found at 669 nm (14946 cm^{-1}), 410 (24398), 318 (31414), and 276 (36286), and for the dimeric NiCRPc a degenerate band was observed at 672 nm (14887 cm^{-1}) and 632 nm (15832 cm^{-1}), which indicates that the splitting (the difference of two A's in Fig. 4B) is ca. 950 cm^{-1} , while the pair of Soret (B) bands were separated by ca. 2180 cm^{-1} (the difference of two A's at the left-hand side in Fig. 4C). Faraday A terms which indicate the presence of degenerate excited states were also found for the dimer of H_2CRPc at 641 nm (15596 cm^{-1}), 428 (23384), 395 (25309),

336 (29799), and 291 (34388), which gave a value of 1925 cm^{-1} for the separation of the two components in the Soret band region.

Interplanar interactions in the triplet dimers of ZnCRPc and H_2CRPc were examined by time-resolved EPR,¹¹ and compared with those of crowned porphyrin systems. The contributions of charge resonance-type (CR) and exciton-type (EX) interactions were directly estimated on the basis of the zero field splitting parameters of the excited triplet states. The contribution of CR character was largest for the crown-ether-bridged Zn tetraphenyl porphyrin dimer **7** (for the dimer structure, see Fig. 4). This was interpreted mainly in terms of the interaction between the $4p_z$ orbital of Zn and the a_{2u} HOMO of the porphyrin. In contrast, the role of Zn in the ZnCRPc dimer system was estimated to be much smaller, because little interaction was expected between the $4p_z$ orbital of Zn and the a_{1u} HOMO of phthalocyanines (note that the a_{1u} orbital has nodes at pyrrole nitrogens through which the interactions may occur). Furthermore, the S1 (lowest energy excited, singlet state) and T1 (lowest triplet state) energies of monomers and dimers were compared. For the porphyrins, both S1 and T1 were red-shifted, while S1 of CRPc was blue-shifted by dimerization. These observations supported the importance of CR and EX interaction for the Zn porphyrin and ZnCRPc dimer, respectively.

Next, Pc analogues with C_{2v} symmetry containing three crown ether units, **8** and **9** (Fig. 6), were prepared and their properties were examined.¹² From the Pc structure, one benzene unit was removed or fused and the other three benzenes were linked to 15-crown-5 ethers. Differing from tetraphenylporphyrins having three or four crown ether units, the cation-induced cofacial eclipsed dimers can again have C_{2v} symmetry. Since this type of chromophoric system had not been realized previously, this gave us a rare opportunity to study the optical properties of such systems. By the addition of K^+ , Rb^+ , or Cs^+ , cofacial dimerization was induced, as in the case of the MtCRPc with four 15-crown-5 units having D_{4h} symmetry, and the interplanar distance was estimated to be $4.1\text{--}4.2 \text{ \AA}$ from analysis of the EPR spectra of the copper complexes. The electronic and MCD spectra in the absence of these cations showed split Q bands as a result of the lifting of the upper state degeneracy, as shown typically for tribenzotetraazaporphyrin, **8**, in Fig. 7A, while the dimers gave blue-shifted Q bands, as can be deduced from the exciton theory. However, the Q MCD band had a dispersion curve (Faraday A term type) characteristic to the upper state degeneracy corresponding to the absorption peak, indicating that the spectra of cofacial eclipsed dimers are insensitive to the symmetry of the constituting monomer (note that the C_{2v} chromophore cannot have degenerate excited states from the standpoint of group theory).

These ZnCRPc monomers with three crown ether units showed both S1 and S2 (second lowest energy excited, singlet state) emission (Fig. 7B for **8**). The S2 emission was much broader than the S1 emission; in each case the Stokes shift of the S1 emission was very small, while that of the S2 emission was very large. Interestingly, the quantum yield of the S1 emission decreased with decreasing molecular symmetry from a value of 0.16 for ZnPc with a D_{4h} π system to 0.09 for **8** and tribenzomononaphthotetraazaporphyrin, **9**, with C_{2v} chromophores, while the lifetime was longer for larger macrocy-

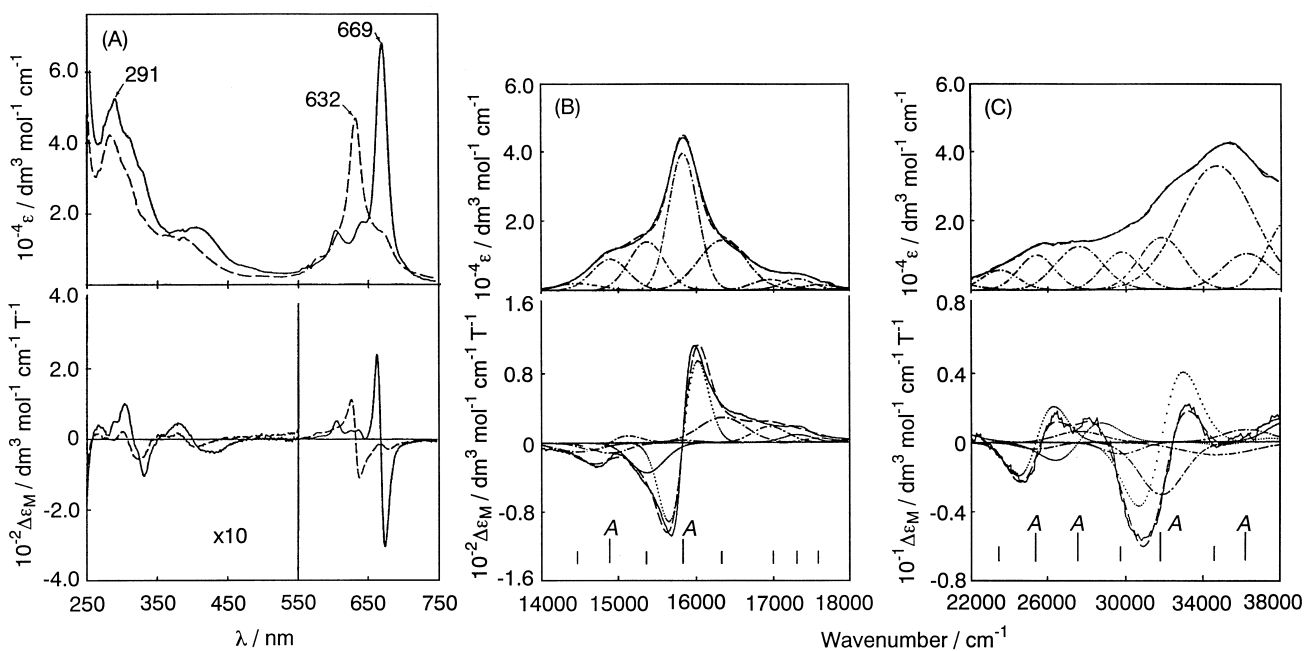


Fig. 5. (A) MCD (bottom) and electronic absorption spectra (top) of NiCRPc monomer (solid lines) and its K^+ -induced dimer (broken lines) in $CHCl_3$. (B) and (C) are band deconvolution analyses of the dimer spectra in the Q and Soret band regions, respectively. "A" denotes the positions of Faraday A terms.

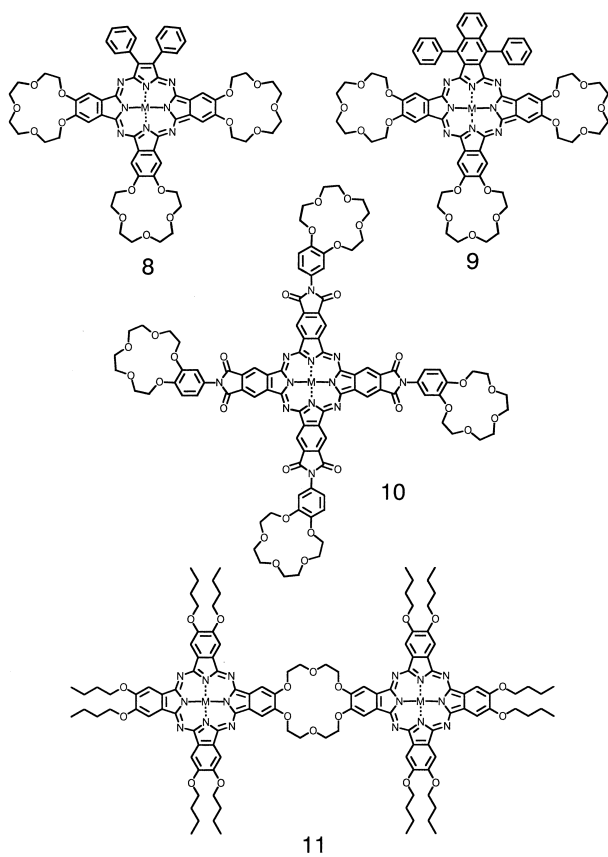


Fig. 6. Pc analogues containing three 15-crown-5 units, **8** and **9**, another type of tetra-crowned **Pc** **10**, and a **Pc** dimer linked peripherally by one 18-crown-6 unit, **11** (Fig. 6), did not show any evidence of dimerization by the addition of various cations.^{14b}

cles, suggesting the operation of mechanisms other than non-radiative decay. On the other hand, the quantum yield of S2 emission is the smallest for the most symmetrical D_{4h} π system and becomes larger for lower C_{2v} π systems.

In contrast to the S1 emission, whose decay curves could be fitted by single exponential curves, double exponential curves were always required for the S2 emission in order to obtain a good fit. Two components, one with τ = subnanosecond and the other with τ = 19–27 ns, were required. Since the latter values were fairly large for states with a singlet multiplicity, it was deduced that the S2 emission may be originating in ligand-centered triplet states, such as $\pi-\pi^*$.

Zero field splitting parameters, D and E , of the Zn complexes with three crown-ether units were obtained by analysis of time-resolved EPR spectra. In the case of the monomers, the D value decreased with increasing molecular size, indicating delocalization of the unpaired electrons over the whole macrocycle. The D value further decreased on cofacial dimer formation. Concerning the predominant intersystem crossing to T_2 (the z component of triplet sublevels) ($P_z \gg P_x, P_y$ (P : population)) which was obtained from simulation of the spectra, participation of the d orbitals (d_{xz}, d_{yz}) of the Zn atom in the T1 ($\pi-\pi^*$) was considered, which would represent a striking contrast to metal-free¹¹ and MgPc¹³ ($P_x, P_y \gg P_z$).

A four crown-ether-linked phthalocyanine prepared from the tetraanhydrides of 2,3,9,10,16,17,23,24-octacarboxyPc and 15-crown-5-ed aniline, **10** (Fig. 6), also showed a two-step three-stage cofacial dimerization, but this process was not as clear as for the above CRPc systems.^{14a} A phthalocyanine dimer linked peripherally by one 18-crown-6 unit, **11** (Fig. 6), did not show any evidence of dimerization by the addition of various cations.^{14b}

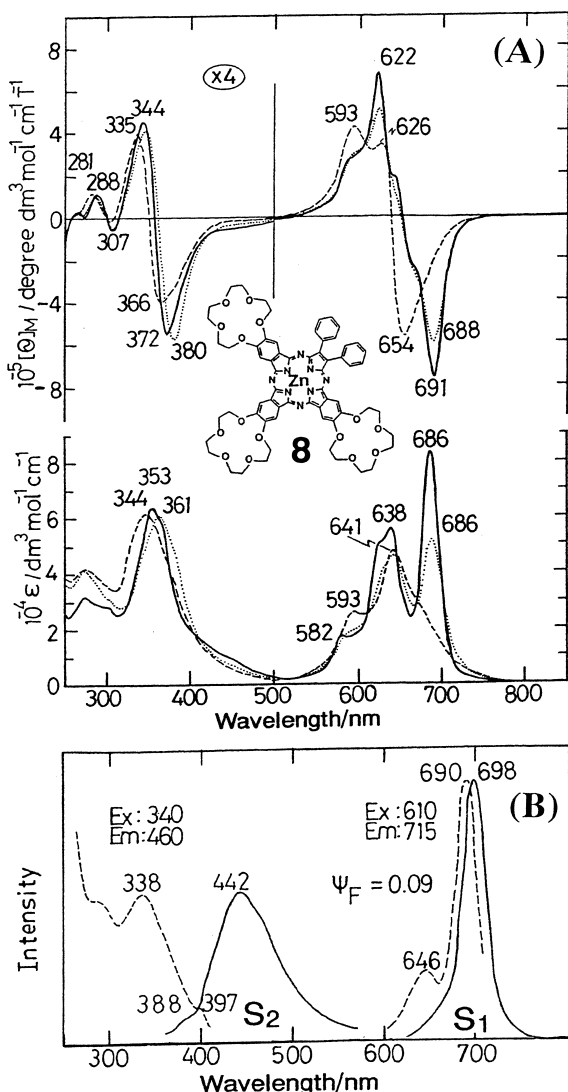


Fig. 7. (A) UV-visible absorption (bottom) and MCD (top) spectra of **8**, monomer (solid lines), **8**–Rb⁺–**8** linear dimer (dotted lines) and [**8**]₂(Rb)₃ cofacial dimer (broken lines) in CHCl₃. A dispersion type MCD curve associated with the Q₀₀ band of [**8**]₂(Rb)₃ suggests that the Q1 state may be degenerate. (B) Fluorescence emission (solid lines) and excitation spectra (broken lines) of **8** in CHCl₃. There is no intensity relationship between the S1 and S2 emissions.

2. Optically Active Phthalocyanines

Optical activity is ubiquitous in nature. In the case of porphyrinic compounds, hemoproteins and chlorophylls have been well known for many years. Synthetic chiral porphyrins have also been reported over the last 20 years or so, but the history of optically active Pcs is only approximately half as long as that of porphyrins. One of the reasons for this appears to be a difficulty in controlling the molecular structure. The first chiral Pcs, **12** (Fig. 8), was reported in 1988;¹⁶ it contained optically active carbons in the side chains and showed mesomorphic behaviour.

2-1. Phthalocyanines with Optically Active Aromatic Molecules. a) Peripheral Substitution. Our first chiral

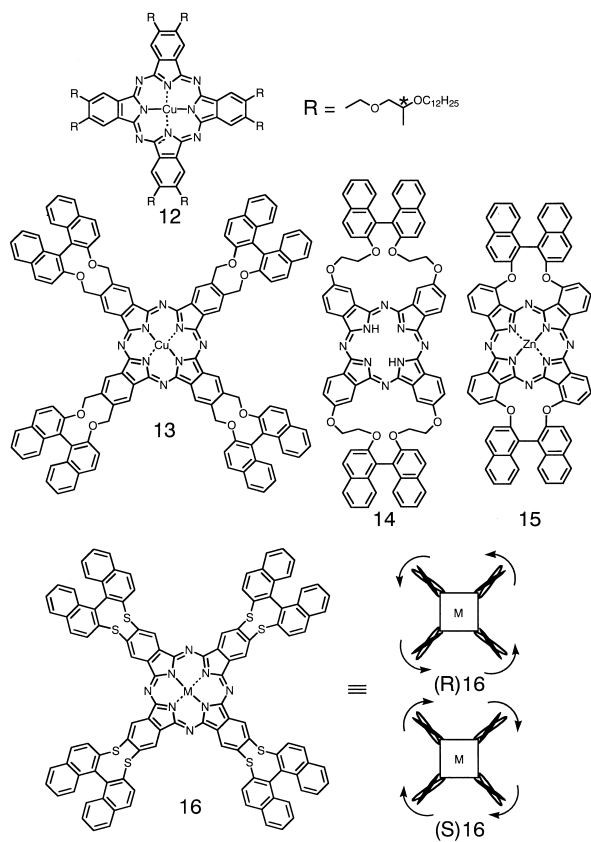


Fig. 8. Structures of the first chiral Pcs, **12**, reported in 1988, our first chiral Pcs, **13** and **14**, reported in 1993, and two types of optically active binaphthyl-linked Pcs, **15** and **16**, used for the elucidation of CD generation mechanism in 1999.

Pcs contained optically active binaphthyl units on the Pcs periphery, **13** and **14** (Fig. 8), and were designed for three purposes. Firstly, we wanted to know the relationship between the helicity and the sign of induced circular dichroism (ICD) in hemoproteins. Hemoproteins generally show either positive or negative CD curves throughout both the Soret and Q band regions, and hence their shape is often similar to that of the absorption spectrum. However, the correspondence between the asymmetric environment surrounding the heme and the sign of the ICD had not been determined. According to theoretical calculations,¹⁷ the ICD sign was determined solely by a coupled oscillator interaction between the heme transitions and allowed π – π^* transitions in nearby aromatic side chains. Therefore, we thought it possible for the Pcs chromophore and chiral binaphthyl units to function in place of the heme chromophore and the nearby aromatic side chains, respectively, in hemoproteins. The second interest was to ascertain whether or not chirality control of the Pcs stacking was possible, since Pcs were well known to be prone to cofacial aggregation. The last aim was to elucidate the generation mechanism of the CD. Since the Q band corresponding to the longest-wavelength allowed transition is much more intense for Pcs than for porphyrins, Pcs were thought to be better for this purpose. Thus, two types of binaphthyl-linked Pcs were synthesized.¹⁸ In one type of precursor, a chiral binaphthyl unit was linked to the 4th and

5th position of phthalonitrile via two two-membered alkyl chains, **13**, and in the other type two phthalonitrile units were bound to hydroxy groups of binaphthyl-2,2'-diol via two four-membered alkyl chains, **14**. The resultant Pcs contained, respectively, four and two binaphthyl units. Four *R* and *S* binaphthyl-linked CuPc, **13**, produced positive and negative CD, respectively, corresponding to the entire region of the absorption spectrum of the Pc chromophore. Since *R* and *S* binaphthyls are left- and right-handed conformers, respectively, it was determined that hemoproteins in the field of left- and right-handed environments produce positive and negative ICD signs, respectively. Pcs with two binaphthyl units, **14**, were used for cofacial dimerization experiments. When dimers were formed, Pcs with *R* and *S* binaphthyls showed negative-to-positive and positive-to-negative CD patterns, respectively, associated with the Q band on going from longer to shorter wavelengths. Thus, chirality control of the Pc stacking was achieved: left-handed and right-handed helix, respectively, for the *R* and *S* binaphthyl-linked Pcs. For elucidation of the CD generation mechanism, similar types of Pc were prepared. However, in order to strengthen the CD intensity and lower the structural flexibility, binaphthyl units were placed as close as possible to the center of the Pc, **15** and **16** (Fig. 8).¹⁹ Perturbation theory provided two predominant mechanisms to induce CD: the Kuhn–Kirkwood coupled oscillator mechanism, and the CD stealing mechanism. In the former mechanism, rotatory strength, R1, can arise if the electronic transition dipoles on the chromophore and on the substituent are skewed. R1 is proportional to $(\mathbf{r}_j - \mathbf{r}_i) \cdot (\boldsymbol{\mu}_j \times \boldsymbol{\mu}_i)$, where \mathbf{r}_j and \mathbf{r}_i are the position vectors of the centers of gravity of the chromophores *i* (in this case, Pc) and *j* (binaphthyl), and $\boldsymbol{\mu}$ is the electronic transition moment. The latter CD stealing mechanism directly transfers rotatory strength from the strongly active substituent to the central Pc transition via dipolar coupling. It requires the transition moments at the two centers to be aligned, since the rotatory strength through this mechanism, R2, is proportional to $\text{Im}(\boldsymbol{\mu} \cdot \mathbf{m}_j)$, where \mathbf{m}_j is the magnetic transition moment of *j*. A possible third mechanism might be via coupling between the magnetic transition moment of the central chromophore and the electronic transition moments of the periphery. In the D_{4h} symmetry group of the unsubstituted MtPc, transitions to both the Soret and Q bands transform as E_u representations, while magnetic transition moments require $E_g + A_{2g}$ symmetries. Hence, neither of the Pc transitions carries an intrinsic magnetic moment. Therefore, this third mechanism was strictly symmetry-forbidden.

All possible couplings were considered (Fig. 9). The two mechanisms which contribute to the rotatory strength of the *B* type transitions were expressed numerically and gave a small negative value, while the induced rotational strength of the *A* component is only due to the CD stealing channel (Fig. 9, top) and gave a large positive value for (*R*)-binaphthylPc. Hence, as a result of superimposition of small negative and large positive branches, the sign of the CD spectrum of (*R*)-binaphthyl-linked Pcs becomes positive in the wavelength region of the Pc chromophore. For the *S* configuration, the sign was, of course, opposite, as was indeed observed (Fig. 10). In the case of four binaphthyl-containing Pcs such as **16**, the shape, particularly the Q band shape, of the ICD spectra was similar to that of the

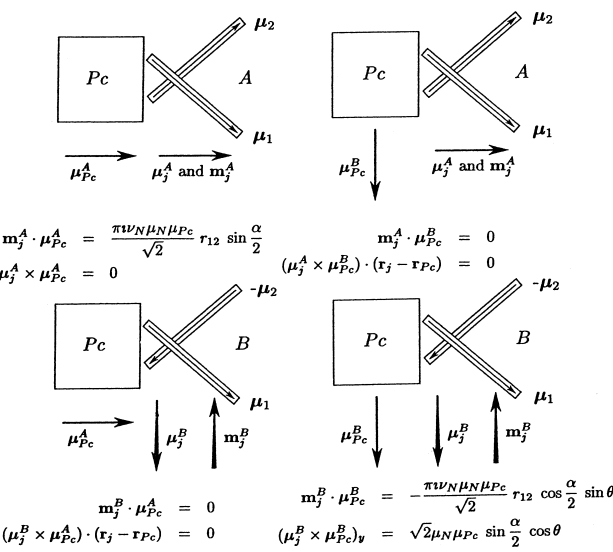


Fig. 9. Overview of all possible couplings. All moments are in-plane except for μ_j^B and m_j^B . Here, α is the angle between the binaphthyl planes, θ is the inclination of the internaphthyl bond with respect to the Pc plane, and r_{12} is the internaphthyl distance.

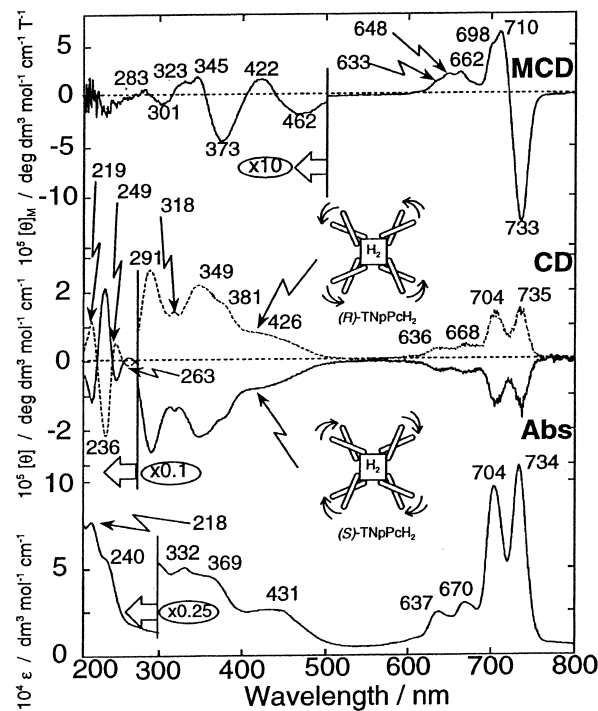


Fig. 10. Spectra for four-binaphthyl-linked H₂Pc.

absorption spectra, since the upper states are degenerate (Fig. 11, left). In the case of two binaphthyl-containing Pcs such as **15** (Fig. 11, right), the shape of the Q absorption and ICD band differed slightly due to the lowering of the Pc chromophore symmetry from approximate D_{4h} to D_{2h} , and concomitant lifting of the upper state degeneracy. Here, a single Q₀₀ absorption band peak in D_{4h} Pc split into a peak at longer wavelength and a shoulder at shorter wavelength, and as a result became broader. In contrast, the Q CD band became sharper. This was

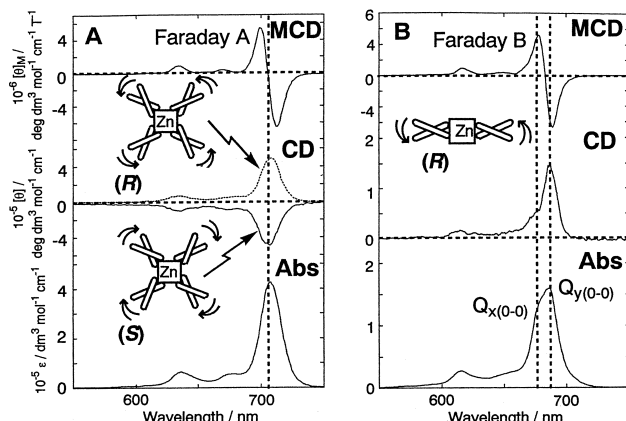


Fig. 11. Electronic absorption (bottom), CD (middle), and MCD (top) spectra in the Q band region of (A) (*R*)- and (*S*)-ZnPc with four-binaphthyl units, and (B) (*R*)-ZnPc with two-binaphthyl units. The MCD and absorption spectra in (A) indicate that the excited state of the Q band is degenerate, while those in (B) suggest it is not degenerate.

interpreted, for example, for the *R*-binaphthyl-linked Pcs, by considering that the Q CD band was composed of the superimposition of a strong positive CD at the Q_{00} absorption peak and a small negative CD corresponding to the shoulder at shorter wavelength. Although the apparent relative intensity of the Soret band to the Q band is stronger for the CD spectra than for the absorption spectra (Fig. 10), a reasonable explanation was provided: this is due to the energy difference between the absorption wavelength of binaphthyls and the Soret or Q bands (see original paper for details).

ICD spectra of electrolysed cobalt species were also recorded.²⁰ Monovalent CoPc generally shows an absorption peak of medium intensity between the Q and Soret band, which has been assigned to a charge-transfer band from the cobalt e_g to ligand b_{1u} orbital under D_{4h} symmetry.²¹ When *R*-binaphthyl-linked CoPc was used, both the starting Co(II) and reduced Co(I) species revealed positive ICD spectra whose shapes were similar to those of the absorption spectra. Since the symmetry of the first excited state is E_u as in the case of the Q and Soret bands, this was taken as an indication that all these bands were in-plane polarized.

The metal-free and the zinc complexes of these optically active Pcs fluoresce from the S1 and S2 states. Since these complexes are chiral, their excitation spectra were recorded using a spectrodichrometer. The resultant spectra are therefore called “fluorescent-detected induced circular dichroism (FDICD)” spectra.²² Pcs with *R*- and *S*-binaphthyl units showed positive and negative spectra, respectively, in the 270–700 nm region which is the absorption window of the Pc chromophore, indicating that the *R* species absorbs left circularly polarized light more than the right, and *vice versa* for the *S* species (Fig. 12). These were the only FDICD spectra ever reported.

b) Axial Substitution. By linking an optically active chromophore as an axial ligand, we can prepare PCs with axial chirality. When we used the reactivity of the axial oxygen in TiOPc, which is readily displaced by *ortho*-phenolic OH groups, with the elimination of water, to produce two ether linkages (i.e. from $\text{Ti} = \text{O}$ to $\text{Ti}(\text{Ar})$),^{23,24} *tert*-butylated

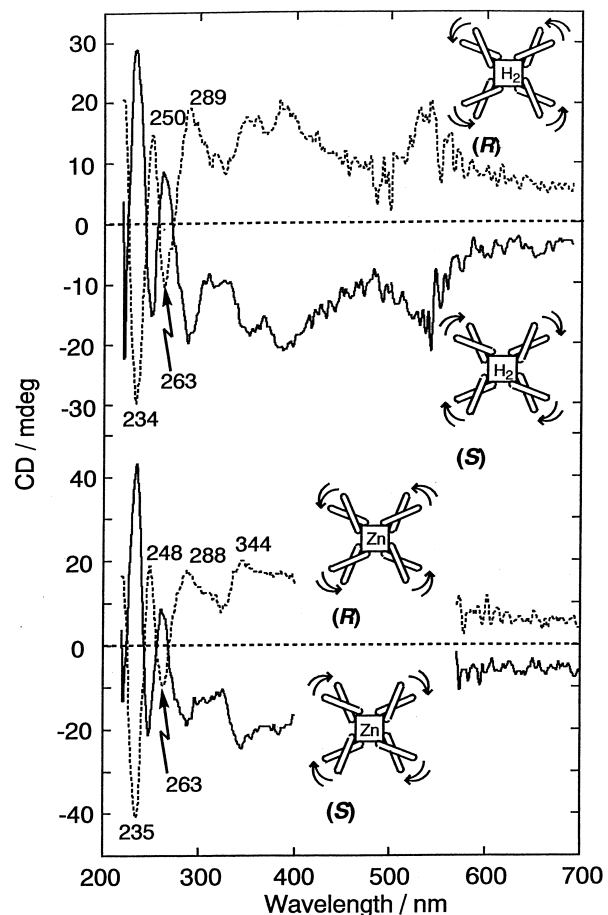


Fig. 12. Fluorescence detected induced CD spectra of (*R*)- and (*S*)-H₂Pc with four-binaphthyl units (top), and (*R*)- and (*S*)-ZnPc with four-binaphthyl units (bottom) in THF.

TiOPc and *S*- or *R*-1,1'-binaphthyl-2,2'-diol were reacted.²⁵ The Q₀₀ band of their absorption spectra split into two peaks due to exciton interaction between the Pc and binaphthyl ligands,²³ while a very weak peak which had not been observed for general Pcs developed at ca. 510 nm (Fig. 13). In the CD spectrum, the *R*-binaphthyl-linked species showed a plus-to-minus pattern at the Q₀₀ and the 510 nm bands, and a small negative-to-strong positive pattern in the Soret band region, viewing from the longer wavelength side. This sign-inversion could only be explained by considering interactions among three independent chromophores (i.e. one Pc and two naphthalenes), since the distance between the Pc and binaphthyl units is too short.

2-2. Phthalocyanines Containing Chiral Carbons in the

Side-Chain. The relationship between the CD sign and configuration of carbons in the side chain has not been reported. One reason is that the CD signals of this type of *Pc* are very weak in intensity. Accordingly, few researchers have been interested in this problem. In order to induce chirality in the *Pc* chromophore, chiral carbons must be located as close as possible to the *Pc* chromophore, preferably without freedom of movement. In order to satisfy these conditions, pyrazinonitrile fused with (1*R*)(*-*)- or (1*S*)(*+*)-camphor was prepared and tetracyclized in the presence of 1,8-diazabicyclo[5.4.0]undec-7-ene (DBU).²⁶ The resultant *R* and *S* metal-free species

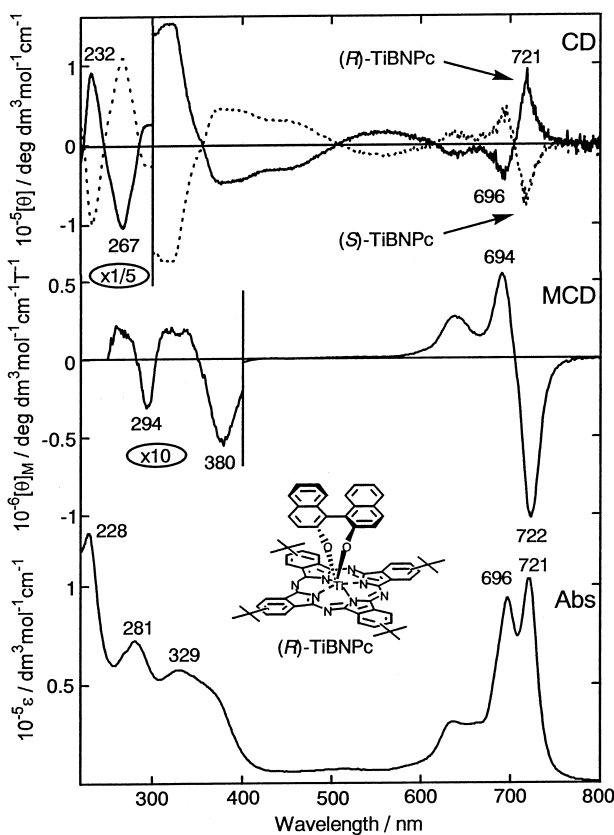


Fig. 13. Structure of *tert*-butylated TiPc linked with a (*R*)-binaphthyl molecule (inset), and absorption (bottom), MCD (middle) and CD spectra (top) of (*R*)- and (*S*)-binaphthyl-linked TiPc in THF.

showed positive and negative CD signs, respectively, throughout all the spectral regions, and the shapes of the CD spectra were similar to those of the absorption spectra. From the result which was described in the preceding section, it was concluded that the chiral carbons in *R* and *S* species gave asymmetric fields of left- and right-handed conformers, respectively. In the case of copper complexes, a dispersion-type CD curve was observed, corresponding only to the Q_{00} absorption band. No reasonable theoretical interpretation has been given for this phenomenon. Copper complexes formed cofacial dimers under a mixed solvent system. Under this condition, the sign of the CD spectrum of the *R* species changed from negative to positive in both the Q and Soret band regions on going from longer to shorter wavelength, while that of the *S* species changed in the opposite manner. These changes in CD sign indicated that the *R* and *S* enantiomers have opposite chirality of stacking: left-handed for the former and right-handed for the latter. Thus, control of the chirality of stacking was attained by changing the configuration of the carbon atoms in the substituents.

2-3. Phthalocyanines with Planar Asymmetry. With the development of synthetic methods,²⁷⁻²⁹ it became possible to prepare tetra-substituted Pcs with single-handed rotation. If an axial ligand is attached, the resultant Pc is a mixture of right-handed and left-handed conformers. Thus, VOPc with single-handed rotation was resolved into two enantiomers by

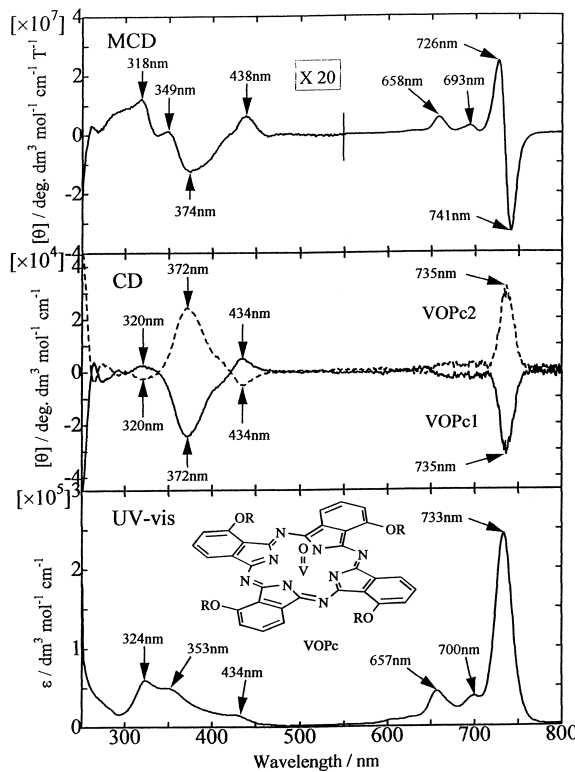


Fig. 14. Electronic absorption (bottom), CD (middle), and MCD spectra (top) of a VOPc with single-handed rotation, in CHCl_3 .

use of an optically active HPLC column, and their CD spectra were recorded (Fig. 14).³⁰ By comparison with the results of theoretical calculations, the second eluted component, which showed positive CD sign at both the Q and Soret bands and negative CD at an $n-\pi^*$ transition band, was assigned to the right-handed conformer (for the structure, see the inset of Fig. 14).

3. Subphthalocyanines

Subphthalocyanine (SubPc), **3** (Fig. 1), was first synthesized³¹ in 1972, and two years later its structure was analyzed using X-ray crystallography.³² In contrast to general Pcs, which have four isoindole units and a planar structure, the SubPc macrocycle is composed of three isoindole units and exhibits a parabolic antenna-like structure, **17** (Fig. 15). However, over the following 15 years no further data were published on SubPcs. When I began studying SubPcs about a decade ago, I aspired to preparing “Red” Pcs, since stable red-dyes and pigments had long been sought for. One idea was to decrease the size of Pcs by removing one isoindole unit, since Pcs having four isoindole units already have a blue-green color. When I manipulated SubPcs which was purplish red, however, it was noticed that quite often metal-free Pcs with a blue color were produced. Since superphthalocyanines which have five isoindole subunits and contain uranium dioxide, and accordingly have a structure which is buckled and severely and irregularly distorted from planarity³³ were known to undergo a ring contraction reaction,³⁴ we considered that SubPc may incorporate another isoindole unit to form the more stable Pcs.

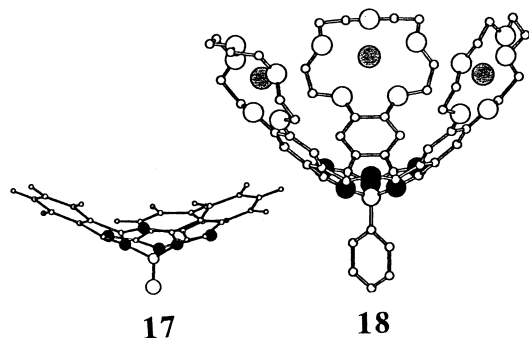


Fig. 15. SubPc **17** (side-view) and crowned SubPc having a phenyl group as an axial ligand **18**. When the latter makes an inclusion complex with 2,6-dimethyl- β -cyclodextrin, the phenyl moiety is trapped into the cavity of 2,6-dimethyl- β -cyclodextrin.

structure. In this way, it was found that the reaction of SubPc with excess isoindole in a mixture of DMSO and aromatic solvent such as chloronaphthalene at 80–90 °C produces mono-substituted type unsymmetrical Pcs and Pc analogues.³⁵ Since then, nearly 50 papers have been published on ring-expansion reactions of SubPcs across the world.^{36,37} We initially thought intuitively that the distorted, strained structure of SubPc is the driving force of the ring expansion. However, our calculations later suggested that the lack of donor–acceptor stabilization in B–N(pyrrole) bonds destabilizes SubPc, and that the initial step of the ring expansion reaction consists of an elimination process of an axial ligand of SubPc.³⁸ In addition, many new SubPc analogues have been prepared and characterized spectroscopically. For example, the axial OH group of SubPcs is reactive and forms a μ -oxo dimer by elimination of a water molecule. A crowned SubPc with an axial phenyl group does not form a cofacial dimer in the presence of cations such as K^+ , Cs^+ , and Rb^+ which induce dimerization of crowned Pcs,^{7,8} because of its bowl-shaped structure, **18** (Fig. 15). However, this crowned SubPc can produce supramolecules with cyclodextrins (CDxs). This was confirmed using NMR and circular dichroism spectroscopy. In particular, the latter spectroscopy has been intensively utilized to determine the orientation of the guest molecule trapped in the cavity of CDx, the polarization direction of the bands of chromophore molecules, and the configuration of two chromophores in the CDx cavity.³⁹ Accordingly, a great deal of information can be obtained from the analysis of circular dichroism spectra of CDx-chromophore supramolecules. Thus, the crowned SubPc with a phenyl axial ligand was found to form a lid-type inclusion complex with dimethyl- β -CDx in both acetonitrile and acetonitrile–water (3:2 v/v), **18** (Fig. 15), but the inclusion of the phenyl group is deeper in the latter solvent.

The electronic absorption and MCD spectra of SubPcs were analyzed by band deconvolution and molecular orbital calculations. As in the case of MPcs, there is only one degenerate excited state in the Q band region, while three degenerate excited states were detected in the Soret band region. In particular, a small Faraday *A* term was perceived at the longer wavelength side of the intense Soret band. This is exactly the same phenomenon as observed for MPcs.⁴⁰ Similarly to the tetraazaporphyrin (TAP),

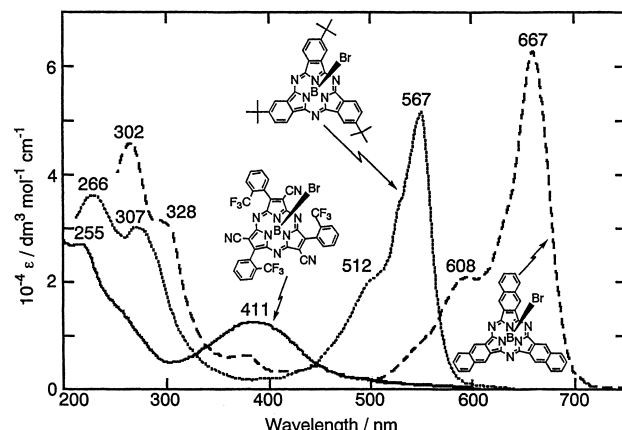


Fig. 16. Electronic absorption spectra of subazaporphyrin (solid line), SubPc (dotted line), and SubNc (broken line) in $CHCl_3$.

Phyrin (TAP), Pc, and naphthalocyanine (Nc) series, the Q band of subazaporphyrin (SubAP), SubPc, and SubNc shifts to longer wavelength with concomitant increase in intensity, while the Soret band shifts to shorter wavelength with concomitant decrease in intensity in this order (Fig. 16). In these compounds, the LUMO is doubly degenerate, and does not change its energy significantly, while the HOMO level destabilizes markedly on going from SubAP, SubPc, and further to SubNc.

SubAP, SubPc, and SubNc all showed S1 emission. In $CHCl_3$, their quantum yields were 0.034, 0.61, and 0.094, respectively, while the Stokes shift of SubAP was particularly large (5900 cm^{-1}) suggesting that the SubAP structure is flexible, and therefore that the structures in the ground and excited states are different. SubPc with crown units alone gave S2 emission in addition to S1 emission. The zero-field splitting parameter, *D*, obtained from analysis of the time-resolved EPR spectrum (0.870 GHz), indicated that the π -delocalization in the T1 state of SubPc is indeed smaller than that of ZnPc (0.705 GHz).

4. Ring-Expanded and Low Symmetrical Phthalocyanine Analogues

When the π -system of tetraazaporphyrins is expanded radially viewing from the center of the macrocycle, Pcs, Ncs, and anthracocyanines (Ac) are formed. However, no one knew the extent of the shift of the Q band and how the Q band intensity would change. In addition, no data were present on low symmetrical Pc analogues when I began studying these compounds around a decade ago. The shape, position, and intensity of the main absorption band of Pc analogues are important factors in considering their role in society, since they have been used as dyes and pigments and in fields utilizing lasers. In order to find the relationship between size, shape, and spectroscopic and/or electrochemical properties, we have prepared several ring-expanded and low symmetrical Pc analogues and characterized these.

a) Symmetrically Ring-Expanded Species. In the first step, TAP, **4** (Fig. 1), Pc, Nc, and Ac having four *t*-butyl groups at similar positions were prepared.^{41,42} Although the Q band shifts to longer wavelength with increasing molecular size, the

extent of the shift becomes smaller the larger the size of the macrocyclic ligand. In other words, if we set the shift from TAP to *Pc* at unity, the shift from *Pc* to *Nc* was 0.7, while that from *Nc* to *Ac* was 0.5. On the other hand, the variation of the absorption coefficient of the Q_{00} band did not have a linear dependence on the size of the chromophore. This increased from TAP to *Pc*, and further to *Nc*, but decreased slightly from *Nc* to *Ac*. Measurements of the redox couples of these compounds showed that the first reduction potential changes only slightly while the first oxidation becomes significantly easier with increasing molecular size, indicating that the LUMO level does not change, while the HOMO level destabilizes markedly on going from TAP to *Ac*. Thus, though the shift of the longest-wavelength band implies a decrease of the HOMO–LUMO gap, the destabilization of the HOMO is the main contributer. These spectroscopic and electrochemical data have been satisfactorily reproduced by molecular orbital calculations within the framework of the Pariser–Parr–Pople (PPP) approximation, except for the absorption coefficient change from *Nc* to *Ac* (in the calculation, the absorption coefficient of the *Q* band of *Ac* is slightly larger than that of *Nc*⁴³). Through these experiments, we obtained a very important result in that *the practical size limitation of the ring-expanded TAP is Ac*, since larger tetraazamacrocycles become more prone to oxidation (after oxidative decomposition, imides such as naphthalimides and anthracimidines are obtained). We also found that the common knowledge that metal-free porphyrins and phthalocyanines have a four-peak *Q* band does not hold for metal-free *Nc* and *Ac* derivatives, since the splitting of the Q_{x00} and Q_{y00} becomes smaller in these species.

In the case of tetrabenzo porphyrin, tetranaphtho porphyrin, and tetraanthracoporphyrin,⁴⁴ the *Q* band shifts to longer wavelength with increasing molecular size, but its position is always shorter, and the relative intensity of the Soret band to the *Q* band is larger than the corresponding tetraazaporphyrins. In contrast to the tetraazaporphyrin series, the first reduction also becomes slightly easier, indicating that the LUMO level becomes slightly lower with increasing molecular size. This is reproduced by PPP molecular orbital (MO) calculations.^{45,46}

Two other types of ring-expanded TAP have been prepared. The first is what we call fluoranthocyanine, **19** (Fig. 17), prepared from fluoranthenedicarbonitrile in the presence of lithium.⁴⁷ In this *Pc* analogue, a five membered aromatic ring fused to 1,8-naphthalene is fused to each benzene ring of *Pc*. The position of the *Q* absorption peak is shorter than that of *Nc*, since only a five-membered ring is fused radially, viewing from the center of the molecule, while the Soret band lies at a longer wavelength than it does for normal *Pcs*. The second is cycloheptatriene-fused TAPs, **20** (Fig. 17).⁴⁸ In these *Pc* analogues, the size and symmetry of the π -system changes reversibly during dehydrogenation/hydrogenation cycling of the cycloheptatriene moiety. Because of the extended π -system, the parent molecules show the *Q* and Soret bands at 710–720 and ca. 400 nm, respectively.

b) Mono-substituted Species. Mono-substituted *Pc* species had previously been prepared by either a mixed condensation method or a polymer support method.⁴⁹ However, the reaction of SubPc with isoindolediimine in DMSO-chloronaphthalene at 80–90 °C led to mono-substituted metal-free species

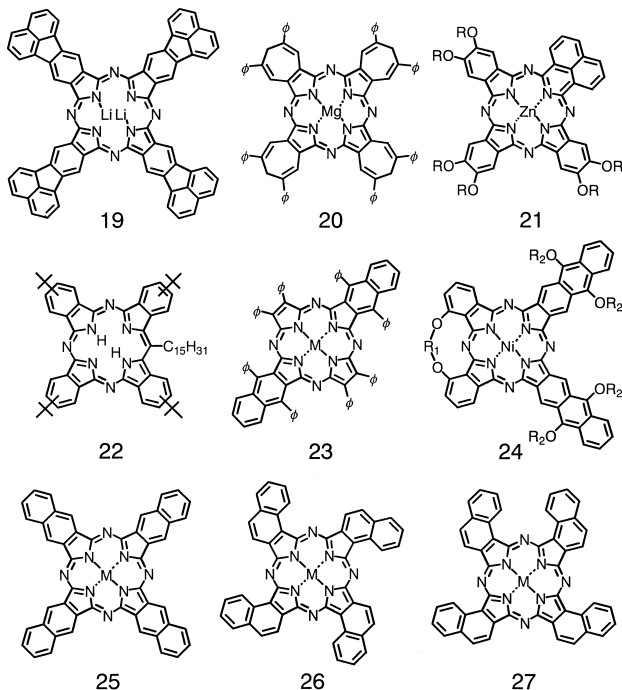


Fig. 17. Structures of ring-expanded and low-symmetrical *Pc* derivatives.

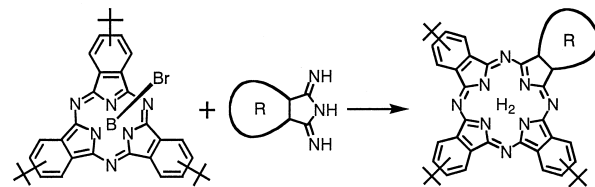


Fig. 18. Ring-expansion of SubPc to produce mono-substituted type *Pcs*. “R” can be aromatic rings such as benzene, naphthalene, anthracene, and pyridine.

in moderate yields (Fig. 18).^{35–38} The stepwise adjustment of the size of the π -conjugated macrocyclic systems became possible by adopting this method. For example, if one reacts succinimidine, isoindolediimine, or benzo- or naphtho-fused isoindolediimine with *tert*-butylated SubPc, the *Q* band positions of the resultant compounds differ by 20–30 nm per benzene unit. By comparing the experimental spectra with the results of PPP molecular orbital calculations, we proposed two pyrrole hydrogen atoms to bind to the nitrogen along the short axis of the molecules.³⁸

In mono-substituted species also, the first reduction potentials are almost constant, irrespective of the size of the introduced aromatic molecule,⁵⁰ but the first oxidation becomes easier with increasing molecular size; these tendencies were reproduced by PPP MO calculations.⁴³ When aromatic molecules of the same size were introduced to the TAP and *Pc* skeletons, the spectroscopic change in the smaller TAP species is larger. Thus, when one benzene molecule was fused to a Co-TAP which has a *Q* band at 615 nm, the *Q* bands appeared at 655 and 634 nm,⁵¹ while when one benzene molecule was fused to a ZnPc which has a *Q* band at 665 nm, the *Q* bands appeared at 693 and 681 nm.⁵² The mono-substituted species

generally shows split Q bands, and the splitting is larger the larger size of the fused aromatics. Interestingly, of the split Q bands, the relative intensity of the band at longer wavelength is always weaker, and this tendency is more marked when larger aromatics are introduced.

Two completely different types of mono-substituted *Pc* analogue have also been prepared. The first is a *Pc* analogue containing a 1,8-naphthalene unit instead of benzene in the *Pc* skeleton, **21** (Fig. 17).⁵³ This compound shows two small absorption peaks beyond the main Q band. The PPP MO calculations suggested that in this type of molecule, the HOMO-1 and HOMO-2 orbitals destabilize, and as a result the HOMO and HOMO-1 levels in *Pc* are inverted. The above unusual absorption bands could be explained using a *five orbital model* (two LUMOs and three HOMOs). Since the spectra of porphyrins and *Pcs* reported to date had all been explained using a four orbital model, this was the first *Pc* analogue whose spectrum could not be interpreted by this model. The other type of mono-substituted *Pc* analogue is tetrabenzotriazaTAP, **22** (Fig. 17) and tetrannaphtho-triazaTAP.⁵⁴ In these compounds, one *meso*-nitrogen in *Pc* or *Nc* is replaced by a carbon atom, so that they therefore lie in between tetrabenzoporphyrin and *Pc* or *Nc*. Compared with the spectra of *Pc* or *Nc*, the Q band occurred at shorter wavelength, while the Soret band was seen at slightly longer wavelength. According to ZINDO/S calculations, the LUMO in *D*_{4h} *Pc* splits into two orbitals and the energy level of the HOMO drops, while that of the HOMO-1 increases in tetrabenzotriazaTAPs. As a whole, the spectra can be interpreted as derivatives of *Pc*. The S1 fluorescence quantum yields of these triazaTAPs were lower than those for the corresponding *Pc* or *Nc*.

Although spectroscopically not very interesting, we developed a transformation method from tribenzo[*b,g,l*]thieno[3,4-*q*]porphyrazine obtained by a cross cyclotetramerization reaction of phthalonitrile and 3,4-dicyanothiophene to mono-substituted *Pc*.⁵⁵

c) Opposite-Di-substituted Species. Our group synthesized the first MPc (a *ZnPc*) with symmetry other than *D*_{4h}.⁵⁶ This was achieved using 3,6-diphenylphthalonitrile as one of two starting phthalonitriles in a mixed condensation. Because of the steric hindrance between the phenyl groups, a *ZnPc* with *D*_{2h} symmetry was preferentially separated, and identified by mass and NMR spectroscopies.

These showed a split, four-peak Q band, similarly to the results for metal-free *Pcs*. In a similar manner, zinc and cobalt dinaphthotetraazaporphyrins with *D*_{2h} symmetry, whose π -conjugated aromatic cores are structural isomers of *Pc*, **23** (Fig. 17) were synthesized from 2,3-dicyano-1,4-diphenyl-naphthalene and 2,3-diphenylmaleonitrile.⁵⁷ Their *D*_{2h} structure was determined from mass and absorption spectra. Comparing the Q band absorption spectra of ZnTAP, mono-naphtho-fused ZnTAP, and di-naphtho-fused ZnTAP, we found that the Q band shifted to longer wavelength with enlargement of the π -system. However, according to symmetry-adapted perturbation theory,⁴³ the energy difference between the Q band of TAP and the center of the split Q bands of di-naphtho-fused TAP should be twice that between the Q band of TAP and the center of the split Q bands of mono-naphtho-fused TAP. In addition, the splitting of the Q bands in *opposite-di*-substituted

species should be more than twice that in mono-substituted species. Therefore, if we collected the portion which yielded the desired mass spectra and these spectroscopic characteristics, these must be the desired *D*_{2h} species. The di-naphtho-fused zinc and cobalt TAPs prepared in this way produced a split Q band at ca. 800 and 640–650 nm and a broad Soret band between 300 and 500 nm, and hence, these compounds can be used as broad light absorbers. Interestingly, the fluorescence quantum yields of both the *D*_{2h} ZnPc and di-naphtho-fused ZnTAP were much lower than that of normal ZnPc with *D*_{4h} symmetry, indicating that the lowering of symmetry reduces the fluorescence intensity, probably through vibrational mode coupling. In voltammetry, the potential difference between the first oxidation and reduction was found to be smaller than that in general *Pcs*, in accordance with the results inferred from the position of the Q band. These *D*_{2h} type MPc species exhibit different behavior even in electrolyzed states.⁵⁸ For example, one-electron reduced MPcs with *D*_{4h} symmetry generally exhibit two intense peaks between ca. 550 and 650 nm which can be assigned to a $\pi^*-\pi^*$ transition from the partially occupied, Jahn-Teller split LUMO $\Delta M_L = \pm 5$ orbitals into the empty symmetrically-split $\Delta M_L = \pm 6$ orbitals in the cyclic polyene model of the electronic structure.⁵⁹ In the case of the one-electron reduced *D*_{2h} type ZnPc, a weak and broad Q band was observed between 600 and 700 nm, with a very broad near-IR band extending to ca. 1000 nm.

d) Adjacent-Di-substituted Species. Our first *adjacent-di*-substituted *Pc* analogue was adjacently di-benzo-substituted CuTAP.⁶⁰ This compound was synthesized because it was expected⁴³ to have a Q absorption band at around 630–640 nm. Indeed, when comparison was made between CuTAP, di-benzo-substituted CuTAP, and a CuPc, the Q band shifted from 586 to 633 and 709 nm in this order, with concomitant increase in intensity. The Q band position of films of this species did not differ practically from that in solution, which is useful in manufacturing read/write compact discs for computers. The potential difference between the first oxidation and reduction was about 1.89 V, which is smaller than that for CuTAP (2.07 V) but larger than for a CuPc (1.70 V). Concerning the shift of the Q band from TAP, to di-benzoTAP, and further to *Pc*, PPP MO calculations suggested a large contribution from the destabilized HOMOs. One notable result from MO calculations on these adjacently di-substituted compounds was that the energy levels of the LUMO and second LUMO are very close. It was found that the thermal stability of the above adjacently di-benzo-substituted CuTAP is approximately 95 degrees lower than the corresponding CuPc having the same substituents. The second example of this series is a dinaphthophthalocyanine with *C*_{2v} symmetry, **24** (Fig. 17), which is a structural isomer of *Ncs* in the sense that eight benzene units are fused to the TAP skeleton.⁶¹ Linearly benzoannulated, so-called, 2,3-*Nc*, **25** (Fig. 17), and angularly benzoannulated 1,2-*Nc*, **26** (Fig. 17), had been known, but no other *Nc* isomers had been reported until two years ago. Our dinaphthophthalocyanine showed Q and Soret bands at ca. 800 and 333 nm, respectively, similarly to normal 2,3-*Ncs*, and a weak broad absorption at around 500 nm, which was assigned to local excitations on the anthracene ring.

As a unique example of an adjacently di-substituted *Pc* ana-

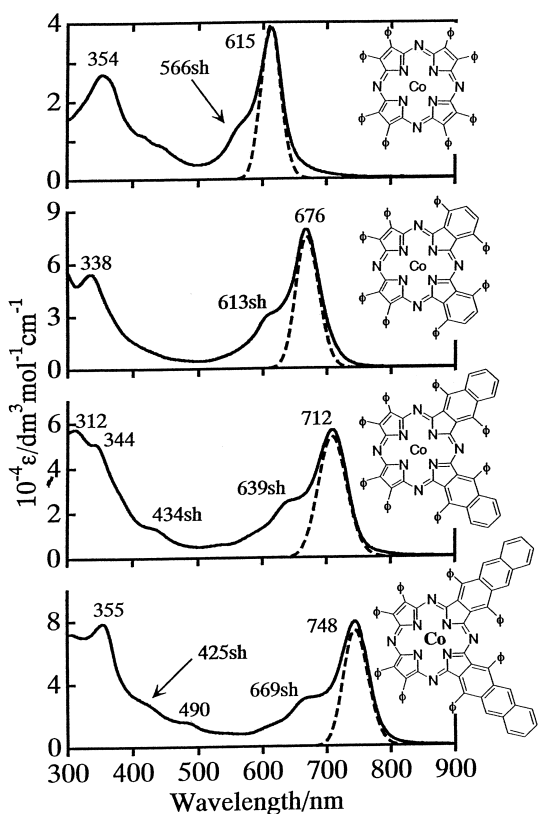


Fig. 19. Electronic absorption spectra of CoTAP and its adjacently di-benzene-, -naphthalene-, and -anthracene-fused derivatives (from top to bottom) in CHCl_3 .

logue, a C_{2v} 1,2-Nc, **27** (Fig. 17), was prepared.⁶² In contrast to 2,3-Nc, the absorption spectrum of 1,2-Nc is closer to that of normal Pcs, although the Soret band appears generally at longer wavelength than for the Pcs. Although the Q state is not degenerate in a strict sense, its Q band did not apparently split, since the splitting was too small (estimated to be ca. 3 nm).

Finally, a series of adjacently di-substituted TAPs were prepared recently.⁵¹ Their Q band shifts to longer wavelengths, without splitting, with increasing molecular size (Fig. 19). As seen in this figure, it became possible to adjust the Q band position between ca. 600 and 750 nm using TAPs.

5. Dimers and Oligomers of Phthalocyanines and Phthalocyanine Analogs

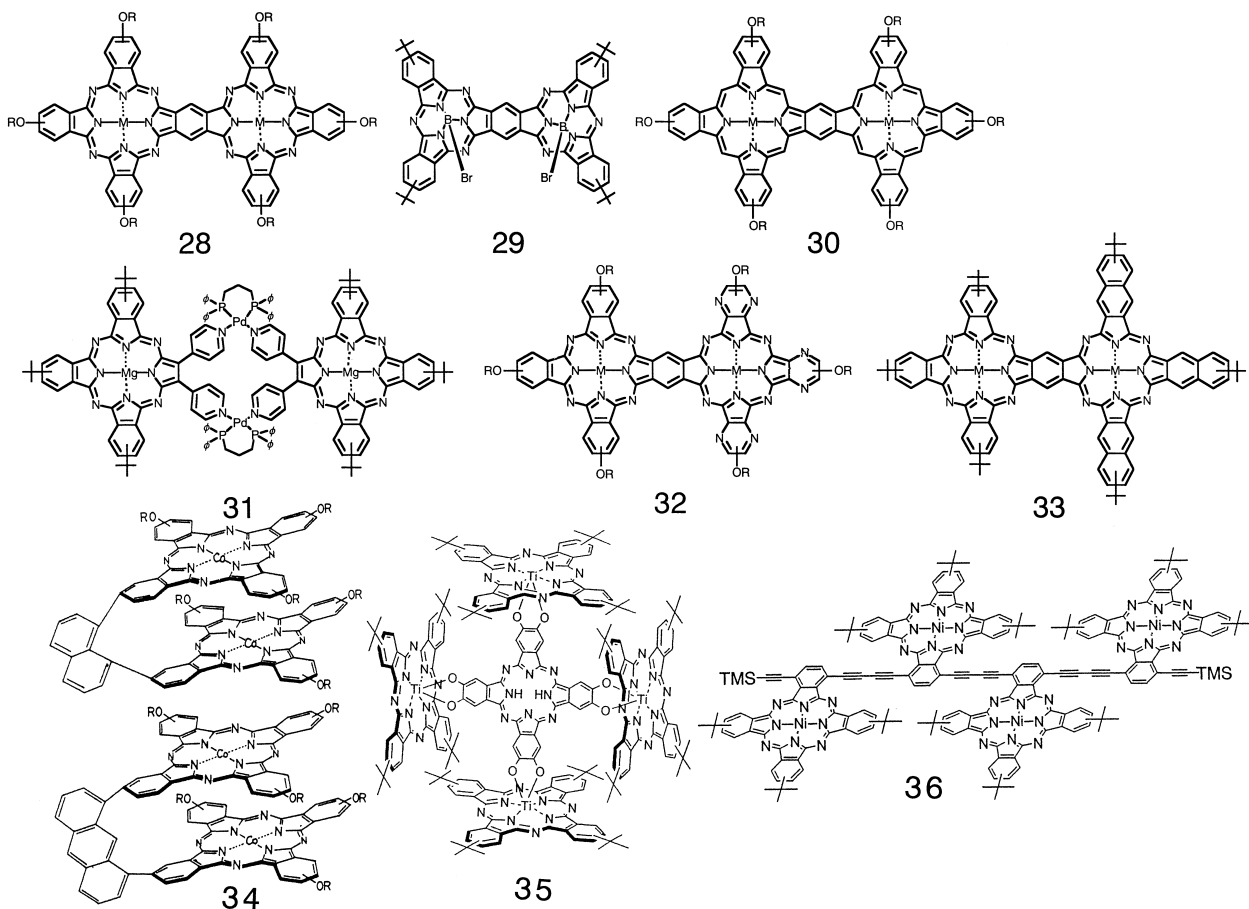
Our objective was to synthesize Pc dimers and oligomers in which the mutual positions of the constituting macrocycles were fixed as far as possible, in order to facilitate the elucidation of interactions. In this sense, cation-induced MCRPcs dimers were exemplary as a cofacial eclipsed dimer. As planar homodimers, M_2PcPcs , **28** (Fig. 20), were first prepared and their properties examined.⁶³⁻⁶⁵ Concerning this type of compound, there was a debate that a common benzene ring connecting two Pc unit might be reduced.^{64b} Indeed Simon's group pointed out the possibility of the existence of two isomeric structures in a study of liquid crystals.^{64c} One isomer was found to form liquid crystals much more easily than the other, and the spectra of this isomer was later found to be consistent with those estimated by MO calculations.^{64a} In any

case, both the first oxidation and reduction and the second reduction couples seen in the corresponding monomer split into two couples in **28**, suggesting that the two constituting units are interacting through dipole–dipole type coupling. Such being the case, we have succeeded in recording the spectra of mixed valence species and in obtaining the comproportionation constants for each redox couple. Analysis suggested that the planarity changes when electrons are added or removed from the system. In order to interpret the electronic absorption spectra of these dinuclear species, MO calculations have been performed within the framework of the PPP approximation, and the absorption and MCD spectra analyzed using a band deconvolution technique (Fig. 21). As inferred from the redox data, all MOs in the corresponding D_{4h} monomer split into two MOs in the dimer; accordingly, these dimer orbitals could be expressed as a linear combination of monomer orbitals (a few frontier orbitals are seen in Fig. 22). In addition, the results obtained by the MO calculations and band deconvolution analysis of the experimental data were in accord with respect to the band position and intensity, strongly suggesting that the interaction in the dimer can be explained by dipole–dipole coupling in each Pc unit (Fig. 21C). Metal-free and zinc derivatives of the dimer showed both S1 and S2 fluorescence emission. The S1 quantum yields of the dimers were roughly an order of magnitude smaller than those of the corresponding monomers, while interestingly the S2 quantum yields of the dimer were always larger than those of the monomer. A reasonable interpretation for the latter phenomenon has not yet been made. In monolayers spread on water, the metal-free complex appeared to have a slipped-stack conformation, tilted from the air–water interface normal plane. In Langmuir–Blodgett films, it may form a slipped-stack molecular arrangement with the stacking axis parallel to the substrate and/or flat-lying conformation on the substrate surface.

In a similar manner, a planar SubPc dimer, **29** (Fig. 20)⁶⁶ and tetrabenzoporphyrin (TBP) dimers, **30** (Fig. 20)⁶⁷ were synthesized. The Q band of the SubPc dimer split into two peaks (separation = 1840 cm^{-1}) and the absorption coefficient decreased. The TBP dimer showed a broadened and slightly red-shifted Q band. Consistent with this, the splitting of the 1st and 2nd oxidation couples of the copper complex were only 110–120 mV.

The first Pc-based dimer assembled via pyridine–Pd–pyridine bridges, **31** (Fig. 20) was prepared recently.⁶⁸ In this case, a tribenzotetraazaporphyrin having two pyridyl groups from the adjacent β pyrrole positions was synthesized first, then this was reacted with a Pd complex having large ligand groups, namely the bis triflate salt of [1,3-bis(diphenylphosphino)propane]palladium. We were not able to use other Pd complexes, because Pd complexes with normal-sized ligands attack not only the pyridyl nitrogens but also the *meso*-nitrogens. According to force field calculations, the two macrocyclic planes are nearly planar, and therefore the use of optically active binaphthyl-substituted Pd complexes produced exciton coupled CD spectra in the Q band region.^{68b} The split Q absorption peaks in the starting monomer split further and shift to slightly longer wavelengths in the dimer.

As planar heterodimers, we have reported two types: a Pc-pyrazinoporphyrazine (PyZ), **32**, type⁶⁹ and a Pc-Nc type, **33**

Fig. 20. Structures of planar dimers and a few oligomers of *Pc* derivatives.

(Fig. 20).⁷⁰ In the preparation of *Pc-PyZ* and *Pc-Nc*, an *ortho*-dinitrile-containing *Pc* was first synthesized from 5,6-dicyano-1,3-isoindolediimine and substituted 1,3-isoindolediimine by mixed condensation, and this was then condensed with an isoindolediimine derivative prepared from a pyrazine and ammonia (*Pc-PyZ*) or with an isoindolediimine derivative prepared from 2,3-dicyanonaphthalene and ammonia (*Pc-Nc*). Both compounds displayed a broad Q band ranging from ca. 600 to 900 nm. No fluorescence was detected from *Pc-PyZ*, plausibly because of intensive intramolecular quenching due to charge-transfer from *Pc* to PyZ moieties (in the case of *Pc-Nc*, S1 fluorescence with a quantum yield about two orders of magnitude smaller than that of the constituting monomer was detected). Because of instability in solution, the redox couples at positive potentials were not clear compared with those of the above homo *Pc* dimers, but the shape of the reduction couples suggested a strong intramolecular dipole–dipole interaction, as seen for the *Pc* homodimer. The zero field splitting parameter of *Pc-PyZ* in the lowest excited triplet state, obtained by time-resolved EPR, showed a contribution from a charge-transfer configuration.⁷¹

Lanthanoid sandwich dimers have also been prepared. For a series of *Pc* complexes,⁷² the first and second oxidation potentials decreased linearly with decreasing ionic radii of the central metals, while the reduction potentials showed no observable change. *Lu(PyZ)₂* dimer showed well-split Q band and Faraday A terms, clearly indicating that the two split Q bands

can both be ascribed to transitions to the degenerated excited state.⁷³ Due to the electron-withdrawing property of the pyrazine rings, all redox couples of *Lu(PyZ)₂* were shifted to anodic potentials by ca. 0.4–0.7 V, suggesting that *Lu(PyZ)₂* can act as a π acceptor. Electrochemistry was performed on two types of *EuNc₂*, and results were compared with that of the corresponding *EuPc₂*.⁷⁴ Due to having a larger π system than *Pcs*, which generally show four redox couples, they exhibited seven ring-based redox couples. Assignment of the bands was attempted using the results of spectroelectrochemistry and simultaneous band deconvolution analysis of the electronic absorption and MCD spectra.

Cofacial *Pc* dimers linked by 1,8-naphthalene- or -anthracene bridges, **34** (Fig. 20) have been prepared, and their spectroscopic and electrochemical properties examined.^{75–77} These compounds were mixtures of *syn* and *anti* isomers, which was reflected in the electronic absorption and MCD spectra and electrochemistry. The Q bands were broad as a result of exciton coupling interaction. The ligand oxidation couples split by ca. 150–200 mV, while the Co(II/I) couples split occasionally by 390–480 mV, so that comproportionation constants were calculated and the spectra of mixed-valence species were recorded. It was found that, when one Co is divalent while the other Co is monovalent, the extra Co electron delocalizes over the two *Pc* rings.⁷⁶ In addition, comparison of results of this study with those of the 1,8-anthracene-pillared diporphyrin⁷⁸ suggested strongly that the interaction of the two

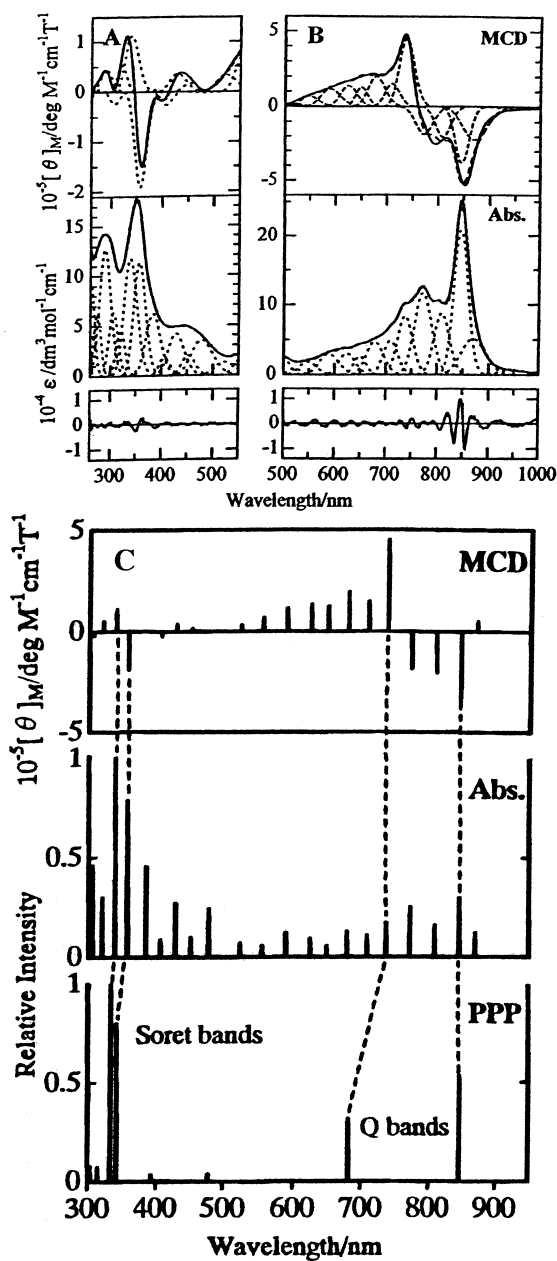


Fig. 21. Band deconvolution analysis of Cu₂PcPc in (A) the Soret and (B) Q band regions. Both the absorption and MCD spectra were fitted with the same band center and bandwidth parameters. (C) is the comparison between the results of the band analysis with those of the PPP MO calculations. Note the good coincidence between the experiments and calculations both in intensity and positions of bands.

rings depends not only on distance but also on the extent of overlap of the electron clouds, since the redox couples of these diporphyrins did not split.

Pcs are prone to aggregation cofacially, but other three-dimensional arrangements are difficult to achieve. We have succeeded in constructing a Pc pentamer consisting of mutually orthogonal Pc units, **35** (Fig. 20), by a one-step reaction using TiOPc and octahydroxy H₂Pc, utilizing the reactivity of the

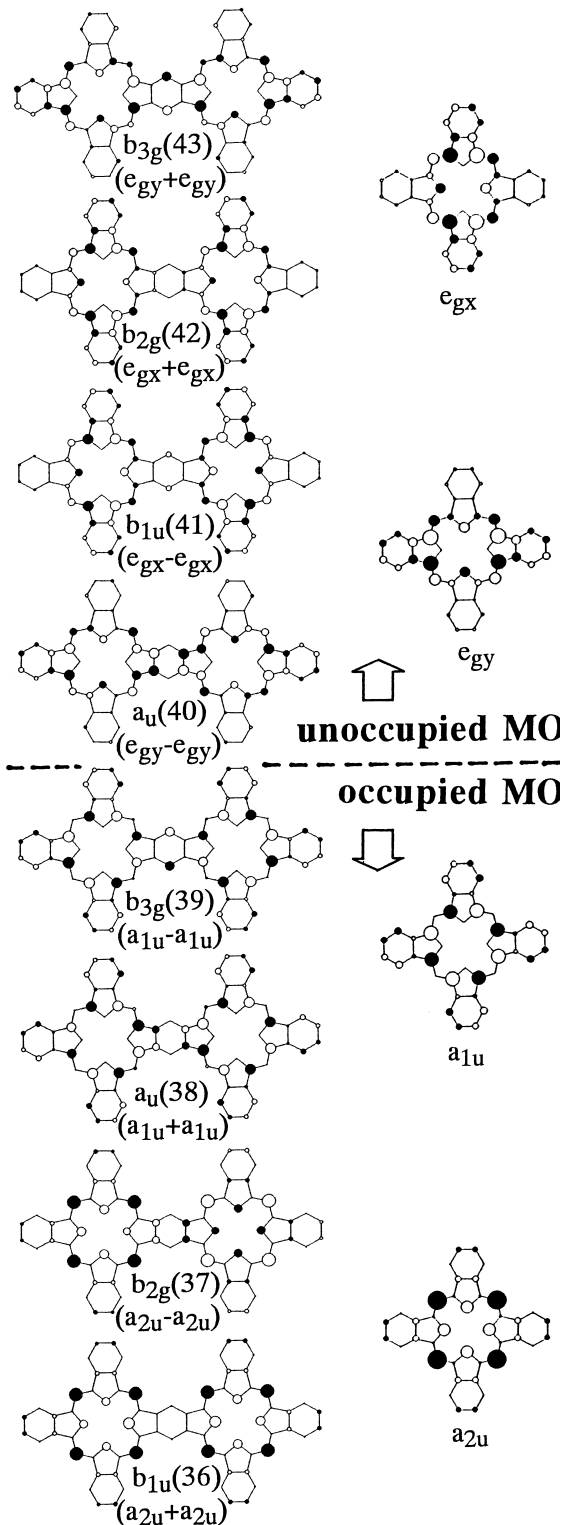


Fig. 22. Eight frontier orbitals of the Cu₂PcPc pentamer and four frontier orbitals of the monomer. Note that the e_{gx} and e_{gy} orbitals are degenerate. The parentheses under each MO of the pentamer indicate the expression of MO using the notation in D_{4h} symmetry which is used for Pc.

axial oxygen of TiOPc.⁷⁹ This pentamer showed a broad Q band, and our calculations on the basis of excitonic theory pre-

dicted four Q-band transitions at 657, 689, 699, and 707 nm, supporting the experimental observations. Linear, carp pentan type *Pc* oligomers, **36** (Fig. 20) have been prepared recently.⁸⁰ Porphyrins cannot take this type of conformation. The electronic absorption spectra of these suggested that the conjugation between the neighboring *Pc* units is not large.

Near-planar heteroleptic oligomers consisting of a *Pc* unit and four porphyrins were prepared in order to show that it is possible to obtain a single isomer of a tetrasubstituted *Pc*.^{81,82} In general, tetra-substituted *Pcs* are mixtures of at least four positional isomers. By reacting amino derivatives of a porphyrin with the tetraanhydride of 2,3,9,10,16,17,23,24-octacarboxy *Pc*, tetra-substituted *Pc* with D_{4h} symmetry was obtained.

6. Electronic State of Iron Phthalocyanines

Under aerobic conditions, the oxidation state of iron in iron porphyrins is generally +3, while that in iron *Pcs* is +2.⁸³ However, we found a few examples of Fe(III)*Pcs* and examined their properties. In particular, these compounds have been used as deodorants over the last 20 years. The Fe(III) state was achieved by simply introducing four or eight electron-withdrawing carboxyl groups onto the periphery of Fe*Pcs*.⁸⁴ Since these compounds aggregate in aqueous solution, the carboxyl group was esterified by alkyl chains, and their properties were examined in organic solvents. Tetracarboxy-esterified Fe*Pc* revealed electronic absorption and MCD spectra characteristic of Fe(III) porphyrins, together with EPR data supporting an Fe(III) high-spin state.⁸⁵ One notable characteristic appeared in the complex formation constants between nitrogenous bases. Namely, the first complex formation constant to form a five-coordinate complex was much larger than that which forms a six-coordinate complex⁸⁶ (in good contrast, Fe(III) high-spin porphyrins show completely opposite behaviour). In addition, interestingly, the mono-imidazole adduct was low-spin Fe(III) while the di-imidazole adduct was a low-spin Fe(II) complex. This is also different from normal Fe(III) porphyrinic systems. That is, mono-base adducts and di-base adducts are generally Fe(III) high-spin and Fe(III) low-spin complexes, respectively. The facile spin-state transition was observed for octacarboxy-esterified Fe(III) high-spin *Pc* on addition of electrolytes such as tetrabutylammonium chloride and bromide.⁸⁷ This was a phenomenon not seen in porphyrinic systems. Such being the case, we examined the oxidation and spin state of tetrabenzoporphyrinatoiron, which is an intermediary compound between normal porphyrin and *Pc*.⁸⁸ Indeed, it showed intermediary characteristics in the spin- and oxidation states of mono- and bis-base adducts (both were Fe(III) low-spin) and in the magnitude of the complex formation constant with bases. In particular, in a Fe(III) high-spin state, the extent of the dissociation of the axial ligand was much larger than in normal Fe(III) high-spin porphyrins. Thus, in the Fe(III) high-spin Fe*Pc*, the dissociation of the axial ligand is considered to be very large, so that the ligation of bases or bad odors becomes easier.

7. Electrocatalytic Reduction of Oxygen Using Water-Soluble Iron and Cobalt Porphyrins and Phthalocyanines

The electroreduction of oxygen in the presence of porphyrins and phthalocyanines has two important applications. The

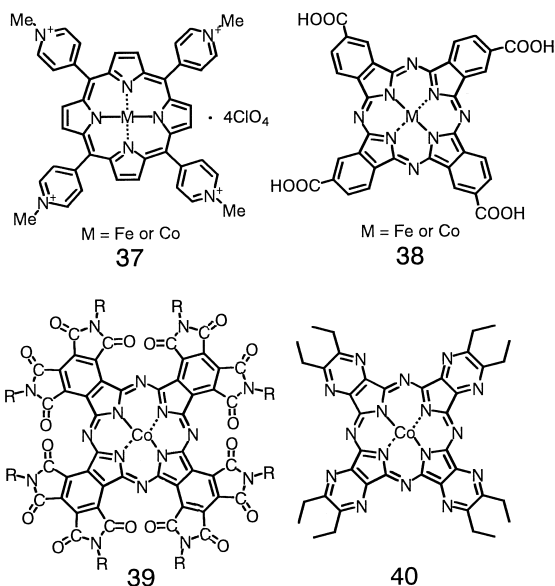


Fig. 23. Structures of catalysts used for the electroreduction of oxygen.

first is as a model reaction of cytochrome oxidase which reduces oxygen to water at the end of the respiratory chain⁸⁹ and the second is as an attractive candidate for the cathode reaction of fuel cells. In particular, Jasinski's discovery in 1964 that Co*Pc* catalyses oxygen reduction at a potential close to that at platinum⁹⁰ provoked a large amount of research in the latter field. However, the exact details of the reaction, such as mechanisms, rates, efficiency, and the structure of the active catalysts, had not been elucidated when we began research in this field. Since the reaction had been carried out in water, we felt that the use of water-soluble catalysts might help elucidate these points. Although several types of porphyrin⁹¹ and *Pc*⁹² were used, the structures of some representative catalysts are shown in Fig. 23. The most exemplary data were obtained for what we call the tetramethylpyridylporphyrin iron complex, **37** ($M = Fe$) (Fig. 23). The oxygen reduction occurred at the potential where the iron was reduced from Fe(III) to Fe(II), and the four-electron reduction of oxygen was attained when the concentration of the catalyst was sufficiently large. The reduction was explained by an electrochemical catalyst regeneration mechanism via hydrogen peroxide, while the possibility of a direct four-electron reduction path was very low, even by simulation of the cyclic voltammograms.^{91c,e} The active form of the catalyst was determined to be the five-coordinate high-spin iron(II) complex using magnetic circular dichroism and EPR spectroscopy.^{91e,92-94} In contrast, the reduction in the presence of cobalt porphyrin, **37** ($M = Co$) (Fig. 23) was a two-electron reduction to hydrogen peroxide, although the mechanism was the same as with the iron catalyst. When tetracarboxylated Fe- and Co*Pc*, **38** (Fig. 23) were used as catalysts, the reduction was explained by the electrochemical catalyst regeneration mechanism, but the active forms of the catalyst were Fe(II) low-spin and Co(I) low-spin complexes. The reduction products were water in the presence of Fe*Pc*, and mainly hydrogen peroxide in the presence of Co*Pc* (Fig. 24).^{92a,b,d} The oxygen reduction potentials were more negative than for the porphyrin

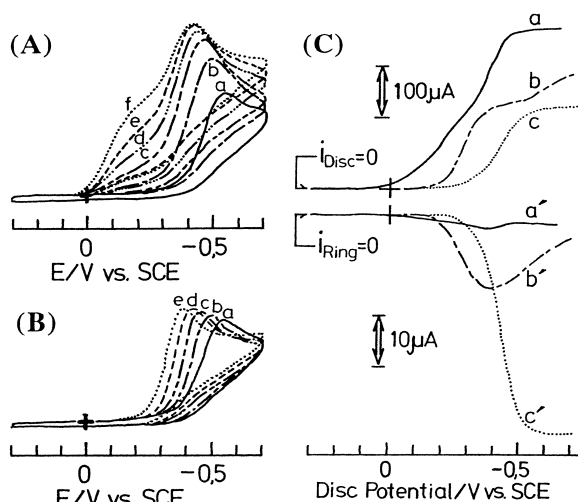


Fig. 24. Cyclic voltammograms for the reduction of O₂ in air-saturated pH 9 solution containing various concentrations of tetracarboxylated (A) FePc or (B) CoPc (solid lines are obtained in the absence of catalysts). In both cases, the reduction potential shifts anodically with increasing catalyst concentration. However, the reduction current increases only in the presence of FePc. (C) Ring-disk *i*-*E* curves for the reduction of O₂ in the presence of tetracarboxylated FePc (curves a and a') or tetracarboxylated CoPc (curves b and b'), and in the absence of catalysts (curves c and c'). The abscissa indicates disk potential and the ring electrode set at +1.1 V detects H₂O₂ as an intermediate of O₂ reduction.

systems, but the durability of the catalysts was better with Pcs. The catalytic ability of the same catalyst was compared in solution and at electrode surface.^{92b} Here, the oxygen reduction potential was more positive when the catalyst was adsorbed on the electrode surface than when it was dissolved in solution, and in the adsorbed case it also depended on the solvent used in dissolving the catalysts. When an octakis(alkyl-imido)Pc cobalt complex, **39** (Fig. 23) was adsorbed onto the surface of electrodes,^{92e} the four-electron reduction of oxygen was attained, which was a quite rare example for cobalt catalysts, since it was commonly thought that oxygen reduction proceeds only to hydrogen peroxide using mononuclear cobalt complexes. The high tendency of the catalyst to aggregate was considered to be the reason for this high efficiency. Oxygen was reduced only to hydrogen peroxide in the presence of cobalt tetrapyrzinoporphyrazine, **40** (Fig. 23).^{92f,i}

8. Concluding Remarks

For people working in national universities, most of the salary and research budget comes from taxes paid by general people living in that country. In this sense, I feel that the research results should be returned to society as far as possible. It was fortunate for me to have been able to work in the field of Pcs, since some results are relatively easily applicable to society. Ferric high-spin Pcs with practical low Fe symmetry, for example, have been utilized as deodorants and anti-bacterial agents, and knowledge on the adjustment of the main band (Q

band) position of Pcs has helped in preparing Pcs which are used in the surface of read/write compact disks. Through research on oxygen reduction using Pcs and porphyrins as catalysts, we were able to deduce to some extent the O₂ reduction mechanism in cytochrome oxidase. This enzyme prevents the accumulation of O₂ in our body, but oxygen may be reduced to water via hydrogen peroxide, the possibility of a direct four-electron path to water being very small. Unfortunately, however, we found simultaneously that Pcs and porphyrins are not robust enough to use as catalysts in fuel cells.

As a researcher in the department of chemistry of a graduate school of science, on the other hand, I had to fulfill the preference of students to work in pure science. Although my research is closely related to society in that the results can be relatively easily returned, what I have done is basic science. For example, the above O₂ reduction is being introduced as a good example of electrocatalysis in an inorganic chemistry textbook used world-wide,⁹⁵ and the analysis of the CD generation mechanism on optically active Pcs has been thought to be one of the most exemplary articles for learning CD spectroscopy. Pcs are a very pertinent subject for learning the relationships between the shape, size, and spectroscopic and electrochemical properties, since there are many variations in symmetry and size. In addition, the development of computer-assisted simulation has enabled to reproduce some experimental data in a short time. The day has come that we can quickly realize what we think.

There are always many capable students in universities. One of our most important roles is to give aspirations to these students through attractive research topics. For countries like Japan which has few natural resources, the only remaining way is to produce a large number of talented people. Hopefully, all university people may feel the same way and do their best in this direction.

The results introduced in this article have been performed with many collaborators. Reports on crown-ether-substituted Pcs have been summarised with Profs. and Drs. Y. Nishiyama and S. Yamauchi of Tohoku University, A. B. P. Lever and C. C. Leznoff of York University, and M. J. Stillman of University of Western Ontario. Research on optically active Pcs were undertaken with Prof. A. Ceulemans of University of Leuven, Dr. W. A. Nevin of Kaneka Co. and Dr. Ishii in my group. We have enjoyed SubPc chemistry with Prof. H. Konami of Kyoto Women's University, while low symmetrical Pcs were prepared by my students, and some analyses and calculations have been carried out in collaboration with Dr. J. Mack of University of Western Ontario. Professor T. Nyokong of Rhodes University has elucidated the electrochemical properties of some sandwich complexes. Mössbauer spectra were recorded by Profs. T. Ohya and M. Sato of Teikyo University, while the electronic states of Fe(III)Pcs were examined in collaboration with Prof. H. Shirai of Shinshu University. 1,2-Nc isomer was studied with Prof. Inabe of Hokkaido University. The results of electrocatalytic reduction of oxygen in the presence of catalysts were published together with Profs. T. Osa of Tohoku University, T. Kuwana of Ohio State University, and Dr. P. Janda of Heyrovsky Institute. The author wishes to express his hearty thanks to all of them for their kind collaborations.

References

1 A. Braun and J. Tcherniac, *Ber. Dtsch. Chem. Ges.*, **40**, 2709 (1907).

2 J. M. Robertson, *J. Chem. Soc.*, **1936**, 1195 ; J. M. Robertson and I. Woodward, *J. Chem. Soc.*, **1936**, 219.

3 "Phthalocyanines—Properties and Applications," ed by C. C. Leznoff and A. B. P. Lever, VCH, Weinheim, New York, Vols. 1–4 (1989, 1992, 1993, and 1996, respectively).

4 "Phthalocyanines—Functions and Chemistry," ed by H. Shirai and N. Kobayashi, IPC, Tokyo (1997).

5 N. Kobayashi and T. Osa, *Heterocycles*, **15**, 675 (1981).

6 V. Thanabal and V. Krishnan, *J. Am. Chem. Soc.*, **104**, 3463 (1982); *Inorg. Chem.*, **21**, 3606 (1982); G. B. Maiya and V. Krishnan, *Inorg. Chem.*, **24**, 3253 (1985); T. K. Chandrashekhar, H. Willigen, and M. H. Ebersole, *J. Phys. Chem.*, **89**, 3453 (1985).

7 A. R. Koray, V. Ahsen, and O. Bekaroglu, *J. Chem. Soc., Chem. Commun.*, **1986**, 932; N. Kobayashi and Y. Nishiyama, *J. Chem. Soc., Chem. Commun.*, **1986**, 1462; R. Hendricks, O. E. Sielcken, W. Drenth, and R. J. M. Nolte, *J. Chem. Soc., Chem. Commun.*, **1986**, 1464.

8 N. Kobayashi and A. B. P. Lever, *J. Am. Chem. Soc.*, **109**, 7433 (1987).

9 M. Kasha, H. R. Rawls, and M. A. Et-Bayoumi, *Pure Appl. Chem.*, **11**, 371 (1965).

10 Z. Gasyna, N. Kobayashi, and M. J. Stillman, *J. Chem. Soc., Dalton Trans.*, **1989**, 2397.

11 R. Miyamoto, S. Yamauchi, N. Kobayashi, T. Osa, Y. Ohba, and M. Iwaizumi, *Coord. Chem. Rev.*, **132**, 57 (1994).

12 N. Kobayashi, M. Togashi, T. Osa, K. Ishii, S. Yamauchi, and H. Hino, *J. Am. Chem. Soc.*, **118**, 1073 (1996).

13 K. Akiyama, S. Toro-Kubota, and Y. Ikegami, *Chem. Phys. Lett.*, **185**, 65 (1991).

14 a) N. Kobayashi, T. Ohya, M. Sato, and S. Nakajima, *Inorg. Chem.*, **32**, 1803 (1993). b) N. Kobayashi, M. Opallo, and T. Osa, *Heterocycles*, **30**, 389 (1990).

15 a) K. Konishi and T. Aida, *Kagaku Kikan Sousetsu*, ed by Chemical Society of Japan, Gakkai Shuppan Center (1997), Vol. 31, p. 99. b) H. Ogoshi and T. Mizutani, *Kagaku Kikan Sousetsu*, Ed. Chemical Society of Japan, Gakkai Shuppan Center, **31**, 109 (1997).

16 I. Cho and Y. Lim, *Mol. Crys. Liq. Cryst.*, **154**, 9 (1988).

17 M. C. Hsu and R. W. Woody, *J. Am. Chem. Soc.*, **93**, 3515 (1971).

18 N. Kobayashi, Y. Kobayashi, and T. Osa, *J. Am. Chem. Soc.*, **115**, 10994 (1993).

19 N. Kobayashi, R. Higashi, B. C. Titeca, F. Lamote, and A. Ceulemans, *J. Am. Chem. Soc.*, **121**, 12018 (1999).

20 N. Kobayashi, *Coord. Chem. Rev.*, **221/222**, 99 (2001).

21 W. A. Nevin, W. Liu, S. Greenberg, M. R. Hempstead, S. M. Marcuccio, M. Melnik, C. C. Leznoff, and A. B. P. Lever, *Inorg. Chem.*, **26**, 891 (1987).

22 N. Kobayashi, The 62nd Okazaki Conference, January 10–13, 1999, Okazaki, Japan, Abstr. P58.

23 N. Kobayashi, A. Muranaka, and K. Ishii, *Inorg. Chem.*, **39**, 2256 (2000).

24 N. Kobayashi and A. Muranaka, *Chem. Commun.*, **2000**, 1855.

25 a) N. Kobayashi and A. Muranaka, The 50th Annual Meeting of the Coordination Chemistry Society, Kusatsu, Japan, September 16–18, 2000. b) A. Muranaka and N. Kobayashi, 8th International Conference on Circular Dichroism, Sept. 23–28, 2001, Sendai, Japan. Abstr. P12.

26 N. Kobayashi and W. A. Nevin, *Chem. Lett.*, **1998**, 851.

27 C. C. Leznoff, M. Hu, C. R. McArthur, Y. Qin, and J. E. van Lier, *Can. J. Chem.*, **72**, 1990 (1994).

28 K. Kasuga, M. Kawashima, K. Asano, T. Sugimori, K. Abe, T. Kikkawa, and T. Fujita, *Chem. Lett.*, **1996**, 867.

29 V. N. Nemykin, N. Kobayashi, V. M. Mytsyk, and S. V. Volkov, *Chem. Lett.*, **2000**, 546.

30 a) F. Narita, Master Thesis, Tohoku University, 1998. b) N. Kobayashi, The 24th International Symposium on Macroyclic Chemistry, July 18–23, 1999, Barcelona, Spain, Abstr. OS2-1.

31 A. Meller and A. Ossko, *Monatsh. Chem.*, **103**, 150 (1972).

32 H. Kietaibl, *Monatsh. Chem.*, **105**, 405 (1974).

33 V. W. Day, T. J. Marks, and W. A. Wacher, *J. Am. Chem. Soc.*, **97**, 4519 (1975).

34 T. J. Marks and D. J. Stojakovic, *J. Am. Chem. Soc.*, **100**, 1695 (1978).

35 N. Kobayashi, R. Kondo, S. Nakajima, and T. Osa, *J. Am. Chem. Soc.*, **112**, 9640 (1990).

36 N. Kobayashi, *Senryo to Yakuhin* **41**, 312 (1996).

37 N. Kobayashi, *J. Porphyrins Phthalocyanines*, **3**, 453 (1999).

38 N. Kobayashi, T. Ishizaki, K. Ishii, and H. Konami, *J. Am. Chem. Soc.*, **121**, 9096 (1999).

39 N. Kobayashi, A. Ueno, and T. Osa, *J. Chem. Soc., Chem. Commun.*, **1981**, 340; N. Kobayashi, R. Saito, Y. Hino, A. Ueno, and T. Osa, *J. Chem. Soc., Chem. Commun.*, **1982**, 706; N. Kobayashi, Y. Hino, A. Ueno, and T. Osa, *Bull. Chem. Soc. Jpn.*, **56**, 1849 (1983); N. Kobayashi, R. Saito, A. Ueno, and T. Osa, *Makromol. Chem.*, **184**, 837 (1983); N. Kobayashi, S. Minato, and T. Osa, *Makromol. Chem.*, **184**, 2123 (1983); N. Kobayashi, R. Saito, H. Hino, Y. Hino, A. Ueno, and T. Osa, *J. Chem. Soc., Perkin Trans II*, **1983**, 1031; N. Kobayashi and T. Osa, *Chem. Lett.*, **1986**, 421; N. Kobayashi, X. Zao, T. Osa, K. Kato, K. Hanabus, T. Imoto, and H. Shirai, *J. Chem. Soc., Dalton Trans.*, **1987**, 1801; N. Kobayashi, *J. Chem. Soc., Chem. Commun.*, **1988**, 918; N. Kobayashi and H. Shirai, *Makromol. Chem., Rapid Commun.*, **10**, 447 (1989); N. Kobayashi, *J. Chem. Soc., Chem. Commun.*, **1989**, 1126; N. Kobayashi and T. Osa, *Carbohydr. Res.*, **192**, 147 (1989); N. Kobayashi and H. Shirai, *J. Polym. Sci., Part C, Polym. Lett.*, **27**, 191 (1989); M. Opallo, N. Kobayashi, and T. Osa, *J. Inc. Phenom.*, **6**, 413 (1989); N. Kobayashi and M. Opallo, *J. Chem. Soc., Chem. Commun.*, **1990**, 477; N. Kobayashi and T. Osa, *Bull. Chem. Soc. Jpn.*, **64**, 1878 (1991).

40 T. Nyokong, Z. Gasyna, and M. J. Stillman, *Inorg. Chem.*, **26**, 1087 (1987).

41 N. Kobayashi, S. Nakajima, and T. Osa, *Inorg. Chim. Acta*, **210**, 131 (1993).

42 N. Kobayashi, in "Phthalocyanines: Properties and Applications," ed by C. C. Leznoff and A. B. P. Lever, VCH, New York (1993), Vol. II, Chap. 3.

43 N. Kobayashi and H. Konami, "Phthalocyanines: Properties and Applications," ed by C. C. Leznoff and A. B. P. Lever, VCH, New York (1996), Vol. IV, Chap. 9.

44 N. Kobayashi, W. A. Nevin, S. Mizunuma, H. Awaji, and M. Yamaguchi, *Chem. Phys. Lett.*, **205**, 51 (1993).

45 N. Kobayashi, *Fine Chemicals*, **25**, 63 (1996).

46 N. Kobayashi and H. Konami, *J. Porphyrins Phthalocyanines*, **5**, 233 (2001).

47 N. Kobayashi, Y. Yoshikawa, O. Ito, H. B. Goodbrand, and J. Mayo, *Chem. Lett.*, **1998**, 423.

48 N. Kobayashi, T. Nonomura, and K. Nakai, *Angew. Chem.*,

Int. Ed., **40**, 1300 (2001).

49 C. C. Leznoff, in "Phthalocyanines: Properties and Applications," ed by C. C. Leznoff and A. B. P. Lever, VCH, New York (1989), Vol. I, Chap. 1.

50 N. Kobayashi, T. Ashida, and T. Osa, *Chem. Lett.*, **1992**, 1567.

51 T. Fukuda, Master Thesis Tohoku University, 2000.

52 N. Kobayashi, J. Mack, K. Ishii, and M. J. Stillman, *J. Am. Chem. Soc.*, submitted.

53 N. Kobayashi, N. Sasaki, and H. Konami, *Inorg. Chem.*, **36**, 5674 (1997).

54 J. Mack, N. Kobayashi, C. C. Leznoff, and M. Stillman, *Inorg. Chem.*, **36**, 5624 (1997).

55 V. N. Nemykin, A. E. Polshina, and N. Kobayashi, *Chem. Lett.*, **2000**, 1236.

56 N. Kobayashi, T. Ashida, and T. Osa, *Chem. Lett.*, **1992**, 2031.

57 N. Kobayashi, T. Ashida, T. Osa, and H. Konami, *Inorg. Chem.*, **33**, 1735 (1994).

58 N. Kobayashi, R. Kondo, T. Ashida, S. Nakajima, and T. Osa, The 2nd International Symposium on Chemistry of Functional Dyes, Kobe, Aug. 23–28, 1992.

59 J. Mack and M. J. Stillman, *J. Am. Chem. Soc.*, **116**, 1292 (1994).

60 N. Kobayashi, H. Miwa, H. Isago, T. Tomura, *Inorg. Chem.*, **38**, 479 (1999).

61 H. Miwa and N. Kobayashi, *Chem. Lett.*, **1999**, 1303.

62 E. H. Gacho, T. Naito, T. Inabe, T. Fukuda, and N. Kobayashi, *Chem. Lett.*, **2001**, 260.

63 C. C. Leznoff, H. Lam, S. M. Marcuccio, W. A. Nevin, P. Janda, N. Kobayashi, and A. B. P. Lever, *J. Chem. Soc., Chem. Commun.*, **1987**, 699.

64 N. Kobayashi, H. Lam, W. A. Nevin, P. Janda, C. C. Leznoff, T. Koyama, A. Monden, and H. Shirai, *J. Am. Chem. Soc.*, **116**, 879 (1994).

65 a) N. Kobayashi, T. Fukuda, and D. Lelievre, *Inorg. Chem.*, **39**, 3632 (2000). b) D. Lelievre, O. Damette, and J. Simon, *J. Chem. Soc., Chem. Commun.*, **1993**, 939. c) D. Lelievre, L. Bocio, J. Simon, J.-J. Andre, and F. Bensebaa, *J. Am. Chem. Soc.*, **1992**, 114, 4475.

66 N. Kobayashi, *J. Chem. Soc., Chem. Commun.*, **1991**, 1203.

67 N. Kobayashi, M. Numao, R. Kondo, S. Nakajima, and T. Osa, *Inorg. Chem.*, **30**, 2241 (1991).

68 a) N. Kobayashi, A. Muranaka, V. N. Nemykin, *Tetrahedron Lett.*, **42**, 913 (2001). b) A. Muranaka and N. Kobayashi, The 31st Forum on Structural Organic Chemistry, Oct. 27–28, 2001, Yamaguchi, Japan.

69 N. Kobayashi, Y. Higashi, and T. Osa, *J. Chem. Soc., Chem. Commun.*, **1994**, 1785.

70 N. Kobayashi, Y. Higashi, and T. Osa, *Chem. Lett.*, **1994**, 1813.

71 K. Ishii, N. Kobayashi, Y. Higashi, T. Osa, D. Lelievre, J. Simon, and S. Yamauchi, *Chem. Commun.*, **1999**, 969.

72 H. Konami, M. Hatano, N. Kobayashi, T. Osa, *Chem. Phys. Lett.*, **165**, 397 (1990).

73 N. Kobayashi, J. Rizhen, S. Nakajima, T. Osa, and H. Hino, *Chem. Lett.*, **1993**, 185.

74 T. Nyokong, F. Furuya, N. Kobayashi, D. Du, W. Liu, and J. Jiang, *Inorg. Chem.*, **39**, 128 (2000).

75 C. C. Leznoff, H. Lam, W. A. Nevin, N. Kobayashi, P. Janda, and A. B. P. Lever, *Angew. Chem., Int. Ed. Engl.*, **26**, 1021 (1987).

76 N. Kobayashi, H. Lam, W. A. Nevin, P. Janda, C. C. Leznoff, and A. B. P. Lever, *Inorg. Chem.*, **29**, 3415 (1990).

77 N. Kobayashi, Y. Yanagisawa, T. Osa, H. Lam, and C. C. Leznoff, *Anal. Sci.*, **6**, 813 (1990).

78 Y. L. Mest, M. L'Her, J. P. Collman, K. Kim, S. Helm, and N. H. Hendricks, *J. Electroanal. Chem.*, **234**, 277 (1987).

79 N. Kobayashi and A. Muranaka, *Chem. Commun.*, **2000**, 1855.

80 J. Usami, Master thesis, Tohoku University, 1999.

81 N. Kobayashi, Y. Nishiyama, T. Ohya, and M. Sato, *J. Chem. Soc., Chem. Commun.*, **1987**, 390.

82 N. Kobayashi, T. Ohya, M. Sato, and S. Nakajima, *Inorg. Chem.*, **32**, 1803 (1993).

83 a) T. Ohya, N. Kobayashi, and M. Sato, *Inorg. Chem.*, **26**, 2506 (1987). b) T. Ohya, J. Takeda, N. Kobayashi, and M. Sato, *Inorg. Chem.*, **29**, 3734 (1990). c) V. N. Nemykin, A. E. Polshina, E. V. Polshin, and N. Kobayashi, *Mendeleev Commun.*, **2000**, 54. d) V. N. Nemykin, A. E. Polshina, V. Y. Chernii, E. V. Polshin, and N. Kobayashi, *Dalton Trans.*, **2000**, 1019. e) V. N. Nemykin, V. Y. Chernii, A. E. Polshina, E. V. Polshin, and N. Kobayashi, *Eur. J. Inorg. Chem.*, **2001**, 733.

84 N. Kobayashi, H. Shirai, and N. Hojo, *J. Chem. Soc., Dalton Trans.*, **1984**, 2107.

85 N. Kobayashi, M. Koshiyama, K. Funayama, T. Osa, H. Shirai, and K. Hanabusa, *J. Chem. Soc., Chem. Commun.*, **1983**, 913.

86 N. Kobayashi, K. Funayama, M. Koshiyama, T. Osa, H. Shirai, and K. Hanabusa, *J. Chem. Soc., Chem. Commun.*, **1983**, 915.

87 N. Kobayashi, M. Koshiyama, Y. Ishikawa, T. Osa, H. Shirai, and N. Hojo, *Chem. Lett.*, **1984**, 1633.

88 N. Kobayashi, M. Koshiyama, and T. Osa, *Chem. Lett.*, **1983**, 163; *Inorg. Chem.*, **24**, 2502 (1985).

89 N. Kobayashi and T. Osa, *Seibutsu Butsuri (Biophysics)*, **24**, 249 (1989).

90 R. J. Jasinski, *Nature*, **201**, 1212 (1964); *J. Electrochem. Soc.*, **112**, 526 (1965).

91 a) N. Kobayashi, M. Fujihira, K. Sunakawa, and T. Osa, *J. Electroanal. Chem.*, **101**, 269 (1979). b) N. Kobayashi, T. Matsue, M. Fujihira, and T. Osa, *J. Electroanal. Chem.*, **101**, 427 (1979). c) N. Kobayashi, M. Fujihira, T. Osa, and T. Kuwana, *Bull. Chem. Soc. Jpn.*, **53**, 2159 (1980). d) N. Kobayashi, M. Fujihira, T. Osa, and S. Dong, *Chem. Lett.*, **1982**, 575. e) P. Forshey, T. Kuwana, N. Kobayashi, and T. Osa, *Am. Chem. Soc., Advan. Chem. Ser.*, **201**, 601 (1982). f) N. Kobayashi and T. Osa, *J. Electroanal. Chem.*, **157**, 269 (1983). g) N. Kobayashi and Y. Nishiyama, *J. Electroanal. Chem.*, **181**, 107 (1984).

92 a) N. Kobayashi and Y. Nishiyama, *J. Phys. Chem.*, **89**, 1167 (1985). b) N. Kobayashi, F. Ojima, T. Osa, S. Vigh, and C. C. Leznoff, *Bull. Chem. Soc. Jpn.*, **62**, 3469 (1989). c) P. Janda, N. Kobayashi, P. R. Auburn, H. Lam, C. C. Leznoff, and A. B. P. Lever, *Can. J. Chem.*, **67**, 1109 (1989). d) N. Kobayashi and H. Shirai, *J. Polym. Sci., Polym. Chem. Edn.*, **27**, 191 (1989). e) N. Kobayashi, K. Sudo, and T. Osa, *Bull. Chem. Soc. Jpn.*, **63**, 571 (1990). f) N. Kobayashi, K. Adachi, and T. Osa, *Anal. Sci.*, **6**, 449 (1990). g) N. Kobayashi, P. Janda, and A. B. P. Lever, *Inorg. Chem.*, **31**, 5172 (1992). h) N. Kobayashi and W. A. Nevin, *Appl. Organomet. Chem.*, **10**, 579 (1996). i) S. Dong, B. Liu, J. Liu, and N. Kobayashi, *J. Porphyrins Phthalocyanines*, **1**, 333 (1997).

93 N. Kobayashi, M. Koshiyama, T. Osa, and T. Kuwana, *Inorg. Chem.*, **22**, 3608 (1983).

94 N. Kobayashi, *Inorg. Chem.*, **24**, 3324 (1985).

95 D. F. Shriver and P. W. Atkins, "Inorganic Chemistry,"

Oxford University Press, 3rd Ed., Chapter 17.



Nagao Kobayashi was born in January of 1950 in Nagano, where the Winter Olympic Games were held in 1998. He earned Dr of Science in 1978 on the magnetic circular dichroism of peroxidase and catalase and Dr of Pharmacy in 1986 on the electrocatalytic reduction of oxygen using water-soluble porphyrins and phthalocyanines both from Tohoku University. He was appointed as a research associate of the Chemical Research Institute of Non-Aqueous Solutions and subsequently of Pharmaceutical Institute of Tohoku University in 1983 and 1985, respectively. After spending one month as an associate professor of the above Pharmaceutical Institute, he has been a full professor of the Department of Chemistry, Graduate School of Science, Tohoku University since April of 1995. He experienced a visiting professor position in the laboratory of Prof. A. B. P. Lever in Toronto, Canada, during 1986-1987. His research interest is the Chemistry of Phthalocyanines which show interesting spectroscopic (particularly absorption, MCD, and CD spectroscopies) properties, and he is always thinking to return some results to society.